Functional Thin Film Polymers for Biopassivation of Neuroprosthetic Implants

by

W. Shannan O'Shaughnessy

B. S. in Chemical Engineering
University of Houston, 1998

Submitted to the Department of Chemical Engineering
in Partial Fulfillment of the Requirements for the Degree of

DOCTOR OF PHILOSOPHY IN CHEMICAL ENGINEERING
AT THE
MASSACHUSETTS INSTITUTE OF TECHNOLOGY

June 2007

Signature of the Author: .....
Department of Chemical Engineering
May 16th, 2007

Certified by: .....
Karen. K. Gleason
Professor of Chemical Engineering
Thesis Supervisor

Accepted by: .....
William Deen
Professor of Chemical Engineering
Chairman, Committee for Graduate Students

Functional Thin Film Polymers for Biopassivation of Neuroprosthetic Implants

by

W. Shannan O'Shaughnessy

Submitted to the Department of Chemical Engineering
on April 17th, 2007 in Partial Fulfillment of the
Requirements for the Degree of
Doctor of Philosophy in Chemical Engineering

ABSTRACT

Neuroprosthetics is the investigation of methods to control external electronic devices utilizing recorded neuronal firing patterns. These investigations are crucial to the quality of life of quadriplegic patients. Central to this field is the ability to implant neural recording probes within the brain that will remain functional over the life of the patient. In this work, two novel polymeric materials for use in biopassive neural probe coatings have been developed and validated. These polymers are synthesized by initiated chemical vapor deposition to allow conformal, pin-hole free coatings of high aspect ratio neural probe assemblies. The first developed material is an electrically insulating barrier coating for the protection of neural probe assemblies. The polymer, poly(trivinyltrimethylcyclotrisiloxane), has an electrical resistivity of 4×10^{15} Ohm-cm and has been demonstrated to be smooth (RMS roughness < 0.4 nm), adherent to silicon substrates, insoluble, and hydrolytically stable. Long term soak testing under physiological conditions has demonstrated retention of electrical properties for > 1000 days. In addition, initial cytotoxicity testing indicates that the material is biocompatible with PC12 neurons.

The second developed material, poly(pentfluorophenyl methacrylate-co-ethylene glycol diacrylate), was developed as a platform for easy surface functionalization of neural probe coatings with bioactive molecules. Single step chemical modification of this material is possible through nucleophilic substitution with primary amines, groups present in all relevant adhesion peptides. Patterned surface functionalization of this material, through microcontact printing, has been demonstrated along with bulk functionalization with small molecule amines from solution. In addition to material development, a novel methodology for additive patterning of CVD polymer thin films has been created. This technique utilizes microcontact printing of photo-active free radical initiator onto the substrate surface prior to polymer deposition. Features 100μm in scale of poly(cyclohexylmethacrylate) with film thicknesses of > 200 nm have been deposited as verification of this technique.

Thesis Supervisor: Karen K. Gleason
Title: Professor of Chemical Engineering

Acknowledgements

This thesis represents not just my personal efforts, but the combined input of many individuals. My time at MIT has not always been easy, but it has been extremely rewarding thanks in large part to my advisors, friends, and family.

First, I must acknowledge Karen Gleason, my advisor and mentor. An excellent scientist and brilliant fundraiser, Karen has supported and encouraged me throughout the doctoral process. Her consultations have always pointed me in the right direction, and she has demonstrated amazing patience in dealing with the irregularities of my intellectual process. I aspire to her mastery of how to succeed in the scientific community. My thesis committee, Drs. Rubner and Stephanopoulos, also contributed a great deal to my scientific understanding.

I must also thank all of my research collaborators, both formal and informal. Many members of the Gleason lab have contributed to my scientific understanding, but none more so than Kelvin. He was exceptionally generous with his time and wisdom, and is a true friend. Both Shashi and Dan were very helpful when I was just getting going in the Gleason lab, and have also contributed greatly to this work through their willingness to collaborate now that they are professors themselves. Dr. Ken Lau provided excellent input on my research investigations, along with generous donations of his time in helping me to ESEM. Sal has been an exceptional co-investigator, and while he has not yet convinced me to love the A's, I do now hate the Angles. Nuria was also an excellent co-investigator, and without her contributions I would definitely not yet have completed this degree. Thanks are due to Wyatt for his tireless efforts to help others within our lab. Meiling Gao, my first and best undergraduate research assistant, contributed greatly to many of my early investigations. Dr. Dave Edell of Innersea Technology, and his tireless assistant Ying Ping, was instrumental in my understanding of the problem I was trying to tackle. I must also thank Tyler for his input on both technical and professional matters, helping to keep me focused in the right direction.

In addition to those who have helped me professionally, many others have aided me personally. I'd like to thank Joe for helping me keep perspective, and Neil for reminding me why I began on this endeavor. Chris, Joel, and the rest of the members of SteriCoat deserve thanks for motivating me to buckle down through the final tough year of my research. Whenever I've needed to take a break, Gregg and Jake have always assisted in that regard. I'd also like to thank Ben, Ryan, Tina, and the rest of the BPT for the many fun hours at the card table, though I'd probably have been out six months ago if it weren't for you guys.

Many others helped to develop me before my time at MIT. I must thank my parents, especially my mother, for their endless belief in my abilities and their encouragement. I would also like to thank Donald Borque and Dr. Richard Pollard, two exceptional mentors from different stages in my life without whose training and support I never would have made it to grad school in the first place.

Lastly, I thank my wife Ashley. She was the driving force in my application to graduate school, the support system I relied on throughout the process, and the most important influence in my life. Much of what I am I owe to her. I'm sorry about the Westgate studio apartment and I love you.

Table of Contents

List of Figures

Chapter One

Chapter Two

Chapter Four

Chapter Five

List of Tables

Chapter Two

Chapter Three

Chapter Five

Chapter One

Introduction

1.1 Biomaterials for Neuroprosthetic Coatings

The development of materials for biological applications is a broad and ever expanding field of study. Many different materials, including pure organic polymers, organosilicons, fluorocarbons, silanes, along with numerous metals have been explored as biomaterials in the literature [1-15]. These materials have a wide range of applications both experimentally and clinically. Novel materials for interacting with biological systems have shown great utility for the *in vitro* study of biological fundamentals[16]. Medical application based investigations, including experimental studies on the scaffolding of cells for organ models[17, 18], the development of surfaces to resist cell adhesion[19-21], and novel delivery methods for therapeutics have all been enabled through the development of biomaterials[22-24]. One area in which biomaterial development has been crucial for success is in the coating of implantable medical devices. These coatings can act to protect the implanted device, as with insulating coatings on pacemaker leads. Medical device coatings can also be utilized to maximize implant biocompatibility. Examples include surface treatments to increase hemocompatibility[2, 4], anti-throbotic coatings of arterial stents[25, 26], and antimicrobial coatings to prevent biofilm formation[27, 28].

This thesis focuses on the development of biomaterial coatings for one specific class of medical devices, neural probes. Neural implants have unique requirements over many other implantable devices and necessitate additional considerations during coating design. In order to ensure the electrical function of the device, an insulating coating must be applied. However, unlike many implanted medical devices, neural probes must interact with the biological environment directly surrounding them. Neural probes are generally implanted for one of two purposes: recording from firing neurons or stimulating neurons to fire. Both require electrical continuity between active sites on the probe and neurons in the brain. While this is not difficult to establish on implantation, it is extremely difficult to maintain over long periods (>6 months), with generally greater than one third of probe sites no longer recording [29, 30].

Loss of probe utility over time is attributed to a process known as gliosis which occurs after implantation. In response to damage caused by implantation, two groups of cells, known as astrocytes and microglia, react by forming a dense cellular sheath around

the probe [31-33]. This sheath generally varies in thickness from 10-50um, though thicknesses up to 250um have been observed [33]. As the sheath forms, it forces neurons away from the probe, decreasing electrical connectivity and greatly reducing probe functionality. Proximity of the active probe sites to the neurons is vital, not just for continued recording or stimulation, but to distinguish between neurons firing singly versus group action potentials. Often, for applications requiring detailed data analysis such as control of a mechanical prosthesis, probe utility is lost before total loss of electrical connectivity. This response is strongest immediately after implantations as high concentrations of reactive cells are delivered to the area through tears in the vasculature caused by implantation. However, studies also indicate that the glial response continues indefinitely, increasing the density of the sheath, if not its thickness as well. This continued response is attributed to two concurrent processes. First, the astrocyte and microglial cells are present in all normal brain tissue. Therefore, even after healing of the damage caused by implantation, they are in the immediate environment of the implant, and continue to react to its presence. Second, and possibly more important, is that the probe may cause continued damage to surrounding tissues aggravating the glial response repetitively [33]. Differences in mechanical properties between the brain and the probe create micromotions of the probe within brain as the implanted subject moves [34, 35]. These motions in turn create damage due to shear of the probe against the brain tissue. As with initial implantation, this damage results in increased concentration of reactive cells in the vicinity of the probe.

Traditional biomaterials research focuses on materials possessing the bulk properties required for the application, while hoping to minimize any negative interactions with the biological environment. This can be a difficult task as many materials possessing desirable bulk mechanical or electrical properties may not have the most favorable biological interactions, and vice versa. In order to avoid this issue, modern biomaterials often utilize surface modification techniques. Biological interaction with an implanted material generally takes place at less than one nanometer depth on the surface of the material [10]. Therefore, by changing the properties of only a small amount of an implantable material (through either surface modification or deposition of a thin film), both bulk and surface properties of an implant can be optimized.

In coating neural implants, this approach is crucial. Protection of the device electronics requires a coating that is conformal, pinhole free, sterile, and extremely stable upon biological implantation. In addition, as it is desirable to coat both the probe and its associated lead wires simultaneously to reduce the number of possible insulation failure points, a flexible material is necessary. The designed material must also be as electrically resistive as possible in order to minimize coating thickness required to achieve the design resistivity of $\sim 10^{14}$ ohm-cm [36]. However, it is unlikely that a material which possesses all these bulk properties will also have the surface properties necessary to remain stable within the central nervous system. Therefore, the ideal biomaterial for coating neural implants is actually two materials: a bulk insulating polymer for protection of the device and a secondary functional polymer to enable surface modification for the optimization of biological interactions.

1.2 CVD Biomaterials

Many methodologies exist for the creation of thin polymeric films including casting, spin-on, dipping, and chemical vapor deposition (CVD). This work will focus on CVD as it has numerous advantages for the application. CVD polymers are formed by reacting one or more gas phase monomers under vacuum. A solid film is created through adsoption of reacted species onto a cooled substrate. CVD processes can be either activated electrically (through the use of plasma), thermally (through the use of a hot filament), or through UV irradiation. CVD films tend to be uniform and pinhole free, and their thickness can be readily controlled[9, 37]. In addition, CVD films are readily applied to substrates of complex geometry and small dimensionality[38]. This is crucial for the application under consideration as the neural probes possess many microscale features. Solvent based coating processes often encounter problems in attempts to uniformly coat substrates containing microfeatures due to surface tension and capillary effects[37].

CVD process can be utilized to create polymeric films not possible to synthesize in a solvated system. Polymers which are insoluble upon formation, or contain unique combinations of different structural units only achievable through gas phase reaction are examples of these [39, 40]. When deposited under correct conditions, CVD films are isotropic, providing the same material properties in all directions. Certain solvent based

processes (especially spin-on) can result in anisotropic coatings which contain directional variation in bulk properties. This is undesirable for the considered application as electrical insulation should be uniform to optimally protect the probe. Additionally, CVD processes are utilized extensively in the microelectronics industry, and are extremely compatible with the manufacturing process currently utilized for fabrication of the neural probes. Lastly, and perhaps most importantly, entrained solvent is a major cause of irritation and even implant rejection in implantable polymers [12]. As CVD is inherently solvent free, these issues area avoided.

Due to the advantages listed above, the CVD process has been studied extensively for formation of thin film biomaterials. Early work considered the impact of plasma polymerized siloxanes and silanes for increasing biocompatibility. Both Chawla et al. [2] and Ishikawa et al. [4] studied the effect of coating implants with a plasma polymerized siloxane film. Results demonstrated a marked increase in blood compatibility of the implant in both cases. Increased compatibility was demonstrated through both a decrease in platelet attachment to the surface, and a decrease in ADP release from those platelets attached to the surface. ADP release is a marker of platelet-platelet interaction and the beginnings of thrombosis. Cannon et al. [1] performed experiments on the coating of neural probe wires with plasma deposited silazanes. Coatings resulted in increased insulation and an increase in viable recording probe percentage.

Development of CVD biomaterials for the insulation of neural probes has been studied extensively within the Gleason lab. Previous work initially focused on the use of fluorocarbon based polymers, specifically Polytertafluoroethylene (PTFE), asinsulating coatings for neural implants [8, 39, 41]. PTFE had previously been shown to possess many desirable properties including good insulation, long term stability, and good biocompatibility [8, 12, 13]. In his doctoral thesis, S. J. Limb examined polymerization of hexafluoropropylene oxide (HFPO) by continuous plasma enhanced CVD (PECVD), pulsed plasma CVD (PPCVD) and hot filament CVD (HFCVD). For the creation of thin film PTFE coatings, CVD deposition possess an additional advantage over conventional polymerization techniques as PTFE is extremely difficult to process in its solid state. By depositing it directly onto the desired substrate, problems of PTFE solvation can be completely avoided.

Initial coatings created by PECVD of HFPO proved conformal and resistive, but tended to posses a wide variety of carbon moieties (besides the CF_2 moiety of which PTFE is entirely comprised). In addition, they tended to be extremely brittle and showed flaking in certain situations. This was not entirely unexpected, as films created using continuous plasma excitation tend to be extremely crosslinked, and therefore very brittle, due to bombardment by ionized species. Indeed, it has been proposed [42] that continuous ionic bombardment during deposition results in the incorporation of many dangling bonds into the film. These inclusions can result in degradation of film properties over time, especially loss of film resistivity. Consequently, it is necessary to avoid excess ionic bombardment of the film as much as possible.

In order to reduce this crosslinking, and increase CF_2 content of the deposited film, the author explored deposition by PPCVD. By varying the duty cycle of the plasma, the authors hoped to better control the chemistry of the reaction. In continuous plasma CVD, the monomer can be split into many fragments (both ions and neutrals), most of which would not normally be stable. The continuous input of energy from the plasma ensures that these unstable species are present throughout the deposition. The result is a wide variation in species present in the resulting polymer [13, 42, 43]. By contrast, PPCVD limits the number of reaction pathways present. While all manner of species are still created during the plasma excitation phase of the process, the off phase of the duty cycle allows time for the less stable species to quench. This leaves only the more stable, generally neutral, species to react and form the film. While some unstable ions will be incorporated during the plasma excitation phase, the overall composition of the film will be much less dominated by these species. Consequently, the level of crosslinking and ion incorporation can be varied through variation in the plasma duty cycle and the absolute length of the refractory period between pulses [41]. Utilizing PPCVD, the author was able to achieve an increase in CF_2 content from 32% to 62% of total carbon incorporated. Resistivities for these films on flat silicon substrates were tested and showed excellent values in the range of 10^{14} to 10^{15} ohm-cm. In addition, the decrease in crosslinking allowed for deposition of much more flexible coatings (see Figure 1-1 below). It should be noted, however, that the coatings had a high degree of surface roughness and tended to

possess pinhole defects. Only ~1 in 10 films deposited proved continuous enough to be tested for resistivity [44]. In addition, the films did not adhere well to wire substrates.

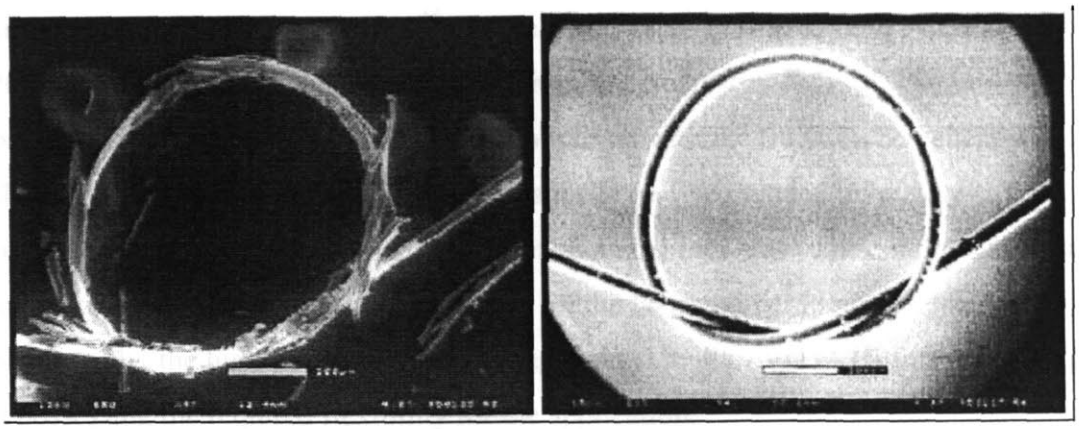

Figure 1-1: Comparison of continuous PECVD (left) and pulsed PECVD (right) coating of 75 μm diameter wires. Loops are 800 μm diameter.

Subsequent to the use of PPCVD, the author then examined HFCVD as a possible method for generating more continuous films with even higher CF_2 contents. The effort was extremely successful in its ability to control reaction chemistry. Through HFCVD, the only reaction path available for the HFPO monomer is decomposition into difluorocarbene and a fluoronated ketone (see Figure 1-2). As the CF_2 diradical is much more reactive than the ketone, films deposited through HFCVD of HFPO consisted entirely of the CF_2 moiety. Indeed, these films were chemically indistinguishable from bulk PTFE [39]. However, as with PTFE created from solution polymerization, the films tended to crystallize easily. The extreme regularity of the PTFE polymer allowed for easy creation of a regular lattice structure, and the resulting films were therefore highly inflexible [45].

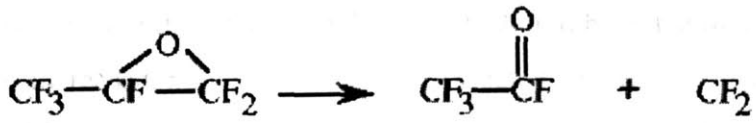

Figure 1-2: Proposed unimolecular decomposition of HFPO

After examining fluorocarbon based CVD films, the group then turned to an exploration of organosilicon based polymers as possible biopassivation coatings. As

noted in section 2.1, organosilicon CVD coatings have shown significant historical promise as biomaterials [2, 4, 5, 12]. In addition, they tend to possess much less surface roughness than fluorocarbon based [15]. Pryce Lewis et al. [11] utilized both PECVD and PPCVD for creation of polymeric coatings from the precursor hexamethylcyclotrisiloxane (D_3). As was observed with the fluorocarbon chemistry utilized by S. J. Limb et al., the PECVD organosilicon films tended to be very crosslinked, and comprised of many different chemical moieties. The continuous plasma excitation provided many reactive pathways for the D_3 monomer to polymerize. Consequently, the high degree of crosslinking created by PECVD of D_3 formed coatings not possessing the required flexibility for the application.

In order to achieve a less damaged, more flexible film, the authors examined PPCVD. Once again, the hope was to limit the number of reaction pathways available from the monomer, and decrease the crosslinking of the deposited film. In the case of D_3 film deposition, the authors hypothesized that the off-time reaction pathways would be limited to those shown in Figure 1-3. A film created entirely by these three reactions would remain flexible as each Si atom would bond in at most three polymer chains [8].

1.	$D_3 \leftrightarrow D_2 + D_1$	*decomposition*
2.	$D_3 \rightarrow Me\bullet + Me_5O_3Si_3\bullet$	*methyl abstraction*
3.	$D_3 \rightarrow l\text{-}D_3$	*ring opening*

Figure 1-3: D3 reaction pathways under PPCVD

Verification of this hypothesis was demonstrated through the creation of PPCVD wire coatings (see Figure 1-4 below). Coatings created with smaller plasma on-time to off-time ratios were significantly more flexible. It should be noted that while film flexibility was increased, no wire coatings were created which were electrically resistive upon flexing. This indicates that the film flexibility achieved was not sufficient for the proposed application. Restive coatings were, however, deposited on flat silicon substrates and shown to have a bulk resistivity on the order of 10^{13} ohm-cm. Additionally, organosilicon based films did not show the pinhole-type failure issues that

fluorocarbon films had, and also displayed superior adhesion especially to silicon based substrates.

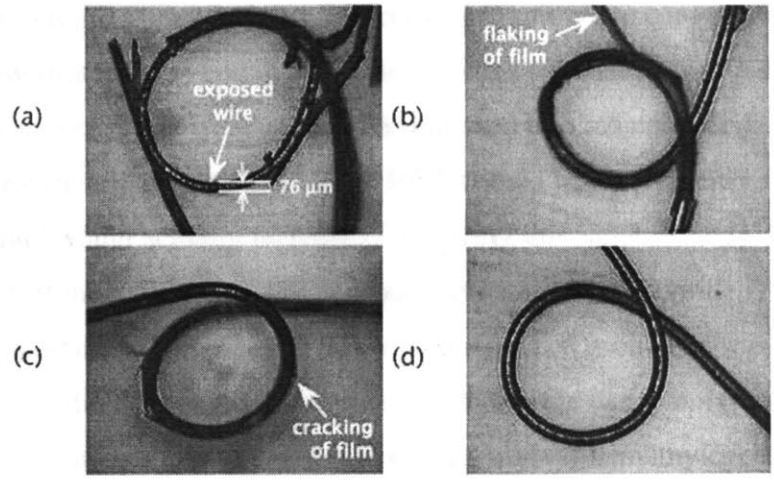

Figure 1-4: Optical micrographs showing 750 µm loops of 3-mil copper wire coated with D_3 pulsed-PECVD film at (a) CW, (b) 10/60, (c) 50/300, and (d) 100/600. Film thickness is (a) 19 µm, (b) 9 µm, (c) 12 µm, and (d) 13 µm. Film deposited at 100/600 shows the most flexibility.

In additional work [46], Price Lewis et al. also explored the HFCVD of both D_3 and octamethylcyclotetrasiloxane (D_4). This work was confined to deposition on silicon flats, and did not address issues of flexibility. It did, however, prove that formation of organosilicon thin films was possible through HFCVD, though at high filament temperatures of 800-1200°C.

Following on from the previous work, organosilicon/ fluorocarbon copolymers were next explored. It was hoped that by combining the two materials into one CVD deposited polymer that the advantages of both classes of material could be utilized, specifically the high resistivity and hydrophobicity of fluorocarbon films and the low surface roughness and conformational properties of organosilicon films.[15]

Initially, an exploration of PPCVD copolymerization was performed. However, it was quickly determined that since HFCVD provided the best control of polymerization chemistry, it was the most likely technique to yield a viable copolymer. HFCVD work first focused on the use of HFPO and D3 as precursor monomers.[47] While it was shown that a copolymeric film containing both CF2 and various silicon moieties was achievable,

the films tended to be highly crosslinked and therefore not flexible enough for the application. All crosslinking appeared to take place through silicon moieties, and many of the crosslinking reaction were driven by the high temperature of reaction (~600°C).

In order to reduce temperature of reaction, and gain more control over reaction chemistry, a new strategy was employed. Price Lewis et al. had shown that by adding a radical initiator (a compound which easily decomposed into radical species) that the filament temperature utilized for HFCVD of HFPO could be significantly reduced, while the deposition rate would actually increase.[48] Utilizing this same strategy, Murthy et al. explored the use of the radical initiator perfluorooctane sulfonyl fluoride (PFOSF) for deposition of copolymeric films. A change in organosilicon monomer was also required as the D_3 monomer did not contain any moieties which were easily polymerized through radical addition. Consequently, the authors selected trivinyl-trimethylcyclotrisiloxane (V_3D_3) as an alternative organosilicon precursor. The vinyl moiety in V_3D_3 provided the required group for radical polymerization of the monomer (see Figure 1-5).

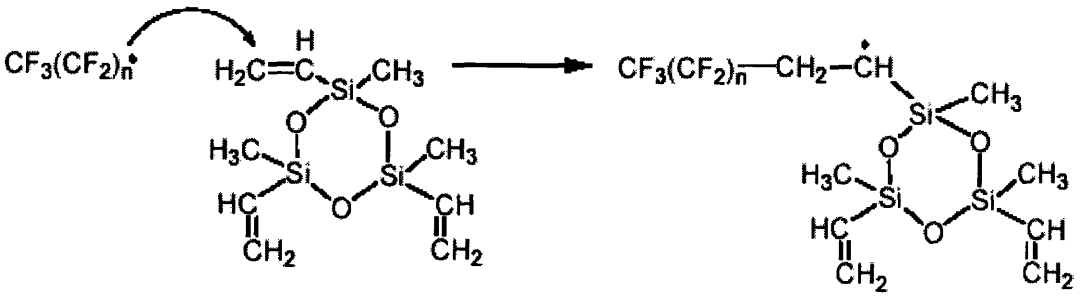

Figure 1-5: Radical Initiation of V_3D_3 polymerization by perfluorooctane sulfonyl fluoride

This precursor chemistry did yield a copolymer as shown in the reactions above. The resulting polymer contained low surface roughness and high hydrophobicity as planned [40]. However, the films contained many flaws, preventing testing of their resistive properties. It was unclear whether the flaws were due to the rapid growth of the film or were the result of metal inclusion from the filament wire. In addition, the films were highly crosslinked through an additional reaction enabled by the initiator which also occurred in the temperature range of the polymerization reaction. This additional

reaction (see Figure 1-6) created silicon moieties bonded to additional chain promoting oxygen atoms, and therefore disallowed the formation of flexible films.

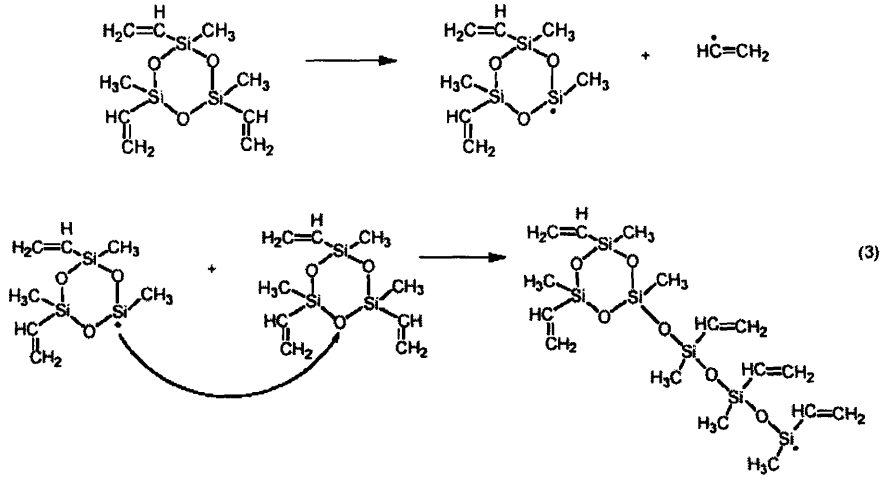

Figure 1-6: Undesirable V_3D_3 side reactions initiated through thermal degradation of the monomer.

1.3 Surface Modification of Biomaterials

Surface modification of biomaterials is often utilized to optimize the surface interactions of a material both *in vitro* and *in vivo*. These modifications can have the added advantage of leaving the bulk material properties, such as electrical resistance or mechanical modulus, of the substrate unaffected. Surface modification can take the form of either physical or chemical changes to the substrate surface. Physical surface modifications can be utilized to influence cell interactions with the material through material modulus[20, 49] or physical patterning[50]. These surfaces can then be utilized to promote cell adhesion (through biomimetic surface roughness)[50], prevent cell adhesion[20, 49], or even sort healthy and diseased cells *in vitro*[51]. Physically patterned surfaces can also be utilized to elicit other biological responses including cell proliferation[50].

Chemical surface modification of biomaterials is even more common than physical. While not focused on flexible coatings, Lahann et al. [52-54] have utilized chemical surface modification of multiple polymers for attachment of cells to both microfluidic devices. Their approach has focused on covalent attachment of biotin to the surface, with subsequent receptor-ligand based attachment of streptavidin. Ligands specific to the desired application, such as fibronectin or laminin, are then non-covalently

bound to the streptavidin for cell attachment within the microfluidic device. Other work in this area is ongoing to look at spatially controlling the growth of neurons on substrates through microprinting of poly-l-lysine [55].

Many CVD based processes for surface modification have been investigated. Chu et al. [13] performed a thorough review of plasma surface modification of biomaterials. In the review, the authors covered multiple processes currently utilized, including ion implantation, plasma grafting, and plasma polymerization. Specific notice was given to polytetrefluoroethylene (PTFE) as a biomaterial. Additional work by Favia & d'Agustino [9] was also detailed, discussing how graft polymerization could be effected on biomaterial substrates through tuning of plasma parameters. This work allowed incorporation of additional moieties (in this case NH_3) on the surface of the material for better biocompatibility. In recent work from Feng et al. [14], plasma polymerization was utilized to deposit a thin film of the bioactive molecule lysine. Performed completely as a vapor phase process, the lysine was polymerized on the surface of glass slides. Subsequent testing verified that the coated slides showed increased biocompatibility with human nerve cells, creating increased growth and attachment.

In the area of neural implants, a number of different surface functionalization approaches have been proposed in the literature. Cui et al. [31, 56] has performed work coating neural probes with various bioactive polymers. These coatings, deposited from solution, contain engineered proteins proven to attract neural cells. The proteins are chosen specific to the application, and generally consist of fragments of either fibronectin or laminin. The hope is to tether the neural probe to the surrounding tissue in order to avoid excessive motion of the probe relative to the brain. In some work, the authors have gone as far as to tailor the coatings to attract neurons directly to the active electrode sites on the probe. This was attempted by co-depositing a conductive polymer with a bioactive molecule as its counter-ion directly on the electrode site. Preliminary results indicate that neurons are preferentially attracted to the bioactive molecule these sites, though it remains to be seen if any long term benefit will be gained. Additionally, stability of the conductive polymer as a biomaterial remains an issue as well.

In their work, Buchko et al. [34, 35, 57] take a slightly different approach. While also applying a coating of bioactive polymer from solution (still based on a fragment of the

fibronectin molecule), they attempt to vary mechanical properties of their material with coating depth. The hope is to ease the transition in mechanical properties from the very stiff silicon of the probe to the much softer cellular materials of the brain. While it is demonstrated that the materials can be deposited as desired, it again still remains to be seen if there will be a measurable impact on long term viability of sensors coated with these materials. Other methodologies under consideration include coating of the probe with poly-n-lysine, a molecule known to attract neurons, for further anchoring of the probe within the tissues [14, 58], and construction of the probe itself from more flexible, polymeric material in order to minimize the difference in mechanical properties [59]. However, all of the coating methodologies contain a similar flaw. The bioactive polymers listed above do not posses the insulating properties necessary for protection of the neural probe from the biological environment. They would therefore necessitate application on top of a normal insulating coating, and would result in increased thickness of the probe. Probe dimensionality has been demonstrated to have a large effect on damage caused upon implantation [33]. Within previous work in the Gleason lab, Murthy et al. [15] proposed the tethering of bioactive molecules to the surface of the insulating coating. The goal was to gain the additional biocompatibility (which is based primarily on the first few nanometers at the surface of the coating [13]) while avoiding any additional film thickness. Proof of concept for tethering bioactive molecules to organosiliocon-fluorocarbon copolymeric surfaces has been performed, but in vivo efficacy of these modifications are yet to be demonstrated.

1.4 Scope of Thesis

Chapters two through five are structured as journal articles, and can therefore be read as independent works. Each chapter contains an abstract, introduction, experimental section, results and discussion section, and chapter conclusions. Chapter two details the synthesis and chemical characterization of a novel organosilicon polymer, poly(trivinyltrimethylcyclotrisiloxane), for the insulation of neural recording probes. The experimental process for depositing the material by initiated chemical vapor deposition is described, along with the kinetics of this process with respect to both reactor and

substrate temperature. In addition, a synthetic mechanism for the polymer is proposed and spectroscopic evidence for this mechanism presented.

Chapter three details the mechanical and electrical properties of poly(trivinyltrimethylcyclotrisiloxane), along with data on the stability of these properties obtained through long term testing under physiological conditions. Cytotoxicity of the material toward neurons is also investigated and initial biocompatibility demonstrated.

Chapter four presents the synthesis and characterization of poly(pentafluorophenylmethacrylate) and its copolymer with ethylene glycol diacrylate by initiated chemical vapor deposition. Bulk and surface functionalization of this material through single step nucleophilic substitution is also demonstrated, including patterned surface modification through microcontact printing.

Chapter five details a novel methodology for depositing additively patterned thin films of poly(cyclohexylmethacrylate). The process utilizes microcontact printing of photo-active free radical initiators followed by in situ polymer growth by photo-intiated chemical vapor deposition. Parameters critical to the process are detailed and utility in producing microscale additively patterned thin films is demonstrated.

Chapter six contains conclusions associated with each of the previous sections along with suggestions for future work. Lastly, it should be noted that research presented in chapters two through four was supported by the National Institute of Health under contract #NO1-NS2-2347. Additive physical patterning work presented in chapter five was supported by the SRC/Semetech Center for Environmentally Benign Semiconductor Manufacture. In addition, the author wishes to thank both the MRSEC Shared Research facility (supported by the NSF under grant #DMR-9400334) and the Institute for Soldier Nanotechnologies (supported by the US Army under contract DAAD-19-02-D-0002) for use of characterization equipment crucial to the completion of this thesis.

1.5 References

1. Cannon, J. G.; Dillon, R. O.; Bunshah, R. F.; Crandall, P. H.; Dymond, A. M., Synthesis of a Fine Neurological Electrode by Plasma Polymerization Processing. *Journal of Biomedical Materials Research* **1980,** 14, (3), 279-288.

2. Chawla, A. S., Evaluation of Plasma Polymerized Hexamethylcyclotrisiloxane Biomaterials Towards Adhesion of Canine Platelets and Leukocytes. *Biomaterials* **1981,** 2, (2), 83-88.
3. L. L. Hench, E. C. E., *Biomaterials: An Interfacial Approach.* First ed.; Academic Press: 1982.
4. Ishikawa, Y.; Sasakawa, S.; Takase, M.; Iriyama, Y.; Osada, Y., Interaction of Plasma-Polymerized Poly(Organosiloxane) Films with Platelets. *Makromolekulare Chemie-Rapid Communications* **1985,** 6, (7), 495-502.
5. Ratnr, B. D.; Johnston, A. B.; Lenk, T. J., Biomaterial Surfaces. *Journal of Biomedical Materials Research-Applied Biomaterials* **1987,** 21, (A1), 59-89.
6. Limb, S. J.; Gleason, K. K.; Gleason, E. F.; Devaney, L. P.; Edell, D. J., Characterizing Plasma-Polymerized Fluorocarbon Surfaces Used in Device Passivation and Fine Wire Coating. *Abstracts of Papers of the American Chemical Society* **1993,** 206, 199-POLY.
7. Nichols, M. F., The Challenges for Hermetic Encapsulation of Implanted Devices - a Review. *Critical Reviews in Biomedical Engineering* **1994,** 22, (1), 39-67.
8. Limb, S. J.; Gleason, K. K.; Edell, D. J.; Gleason, E. F., Flexible fluorocarbon wire coatings by pulsed plasma enhanced chemical vapor deposition. *Journal of Vacuum Science & Technology a-Vacuum Surfaces and Films* **1997,** 15, (4), 1814-1818.
9. Favia, P.; d'Agostino, R., Plasma treatments and plasma deposition of polymers for biomedical applications. *Surface & Coatings Technology* **1998,** 98, (1-3), 1102-1106.
10. Ohl, A.; Schroder, K., Plasma-induced chemical micropatterning for cell culturing applications: a brief review. *Surface & Coatings Technology* **1999,** 119, 820-830.
11. Lewis, H. G. P.; Edell, D. J.; Gleason, K. K., Pulsed-PECVD films from hexamethylcyclotrisiloxane for use as insulating biomaterials. *Chemistry of Materials* **2000,** 12, (11), 3488-3494.
12. Bhat, S. V., *Biomaterials.* First ed.; Narosa Publishing House: New Delhi, India, 2002.
13. Chu, P. K.; Chen, J. Y.; Wang, L. P.; Huang, N., Plasma-surface modification of biomaterials. *Materials Science & Engineering R-Reports* **2002,** 36, (5-6), 143-206.
14. Feng, X. F.; Zhang, J.; Xie, H. K.; Hu, Q. H.; Huang, Q.; Liu, W. W., The RF plasma polymer of lysine and the growth of human nerve cells on its surface. *Surface & Coatings Technology* **2003,** 171, (1-3), 96-100.
15. Murthy, S. K. Chemical Vapor Deposition and Functionalization of Fluorocarbon-Organosilicon Copolymer Thin Films: Doctoral Thesis in Materials Science. Massachusetts Institute of Technology, 2003.
16. Whitesides, G. M.; Ostuni, E.; Takayama, S.; Jiang, X. Y.; Ingber, D. E., Soft lithography in biology and biochemistry. *Annual Review Of Biomedical Engineering* **2001,** 3, 335-373.
17. Griffith, L. G.; Swartz, M. A., Capturing complex 3D tissue physiology in vitro. *Nature Reviews Molecular Cell Biology* **2006,** 7, (3), 211-224.
18. Sivaraman, A.; Leach, J. K.; Townsend, S.; Iida, T.; Hogan, B. J.; Stolz, D. B.; Fry, R.; Samson, L. D.; Tannenbaum, S. R.; Griffith, L. G., A microscale in vitro

physiological model of the liver: Predictive screens for drug metabolism and enzyme induction. *Current Drug Metabolism* **2005,** 6, (6), 569-591.

19. Lyles, B. F.; Terrot, M. S.; Hammond, P. T.; Gast, A. P., Directed patterned adsorption of magnetic beads on polyelectrolyte multilayers on glass. *Langmuir* **2004,** 20, (8), 3028-3031.
20. Thompson, M. T.; Berg, M. C.; Tobias, I. S.; Rubner, M. F.; Van Vliet, K. J., Tuning compliance of nanoscale polyelectrolyte multilayers to modulate cell adhesion. *Biomaterials* **2005,** 26, (34), 6836-6845.
21. Zhang, Z.; Chao, T.; Chen, S. F.; Jiang, S. Y., Superlow fouling sulfobetaine and carboxybetaine polymers on glass slides. *Langmuir* **2006,** 22, (24), 10072-10077.
22. Nahar, M.; Dutta, T.; Murugesan, S.; Asthana, A.; Mishra, D.; Rajkumar, V.; Tare, M.; Saraf, S.; Jain, N. K., Functional polymeric nanoparticles: An efficient and promising tool for active delivery of bioactives. *Critical Reviews In Therapeutic Drug Carrier Systems* **2006,** 23, (4), 259-318.
23. Wood, K. C.; Chuang, H. F.; Batten, R. D.; Lynn, D. M.; Hammond, P. T., Controlling interlayer diffusion to achieve sustained, multiagent delivery from layer-by-layer thin films. *Proceedings Of The National Academy Of Sciences Of The United States Of America* **2006,** 103, (27), 10207-10212.
24. Khandare, J.; Minko, T., Polymer-drug conjugates: Progress in polymeric prodrugs. *Progress In Polymer Science* **2006,** 31, (4), 359-397.
25. Gunn, J.; Cumberland, D., Stent coatings and local drug delivery - state of the art. *European Heart Journal* **1999,** 20, (23), 1693-1700.
26. Bertrand, O. F.; Sipehia, R.; Mongrain, R.; Rodes, J. R.; Tardif, J. C.; Bilodeau, L.; Cote, G.; Bourassa, M. G., Biocompatibility aspects of new stent technology. *Journal Of The American College Of Cardiology* **1998,** 32, (3), 562-571.
27. Norris, P.; Noble, M.; Francolini, I.; Vinogradov, A. M.; Stewart, P. S.; Ratner, B. D.; Costerton, J. W.; Stoodley, P., Ultrasonically controlled release of ciprofloxacin from self-assembled coatings on poly(2-hydroxyethyl methacrylate) hydrogels for Pseudomonas aeruginosa biofilm prevention. *Antimicrobial Agents And Chemotherapy* **2005,** 49, (10), 4272-4279.
28. Nablo, B. J.; Prichard, H. L.; Butler, R. D.; Klitzman, B.; Schoenfisch, M. H., Inhibition of implant-associated infections via nitric oxide. *Biomaterials* **2005,** 26, (34), 6984-6990.
29. Rousche, P. J.; Normann, R. A., Chronic recording capability of the Utah Intracortical Electrode Array in cat sensory cortex. *Journal of Neuroscience Methods* **1998,** 82, (1), 1-15.
30. Kipke, D. R.; Vetter, R. J.; Williams, J. C.; Hetke, J. F., Silicon-substrate intracortical microelectrode arrays for long-term recording of neuronal spike activity in cerebral cortex. *Ieee Transactions on Neural Systems and Rehabilitation Engineering* **2003,** 11, (2), 151-155.
31. Cui, X. Y.; Wiler, J.; Dzaman, M.; Altschuler, R. A.; Martin, D. C., In vivo studies of polypyrrole/peptide coated neural probes. *Biomaterials* **2003,** 24, (5), 777-787.
32. Szarowski, D. H.; Andersen, M. D.; Retterer, S.; Spence, A. J.; Isaacson, M.; Craighead, H. G.; Turner, J. N.; Shain, W., Brain responses to micro-machined silicon devices. *Brain Research* **2003,** 983, (1-2), 23-35.

33. Edell, D. J.; Toi, V. V.; McNeil, V. M.; Clark, L. D., Factors Influencing the Biocompatibility of Insertable Silicon Microshafts in Cerebral-Cortex. *Ieee Transactions on Biomedical Engineering* **1992,** 39, (6), 635-643.
34. Buchko, C. J.; Chen, L. C.; Shen, Y.; Martin, D. C., Processing and microstructural characterization of porous biocompatible protein polymer thin films. *Polymer* **1999,** 40, (26), 7397-7407.
35. Buchko, C. J.; Slattery, M. J.; Kozloff, K. M.; Martin, D. C., Mechanical properties of biocompatible protein polymer thin films. *Journal of Materials Research* **2000,** 15, (1), 231-242.
36. Edell, D., In 2003; p Personal Communication.
37. Pierson, H. O., *Handbook of Chemical Vapor Deposition.* 2nd ed.; William Andrew Publishing: Norwich, N.Y., 1999.
38. Ma, M. L.; Gupta, M.; Li, Z.; Zhai, L.; Gleason, K. K.; Cohen, R. E.; Rubner, M. F.; Rutledge, G. C., Decorated electrospun fibers exhibiting superhydrophobicity. *Advanced Materials* **2007,** 19, (2), 255-+.
39. Limb, S. J.; Labelle, C. B.; Gleason, K. K.; Edell, D. J.; Gleason, E. F., Growth of fluorocarbon polymer thin films with high CF2 fractions and low dangling bond concentrations by thermal chemical vapor deposition. *Applied Physics Letters* **1996,** 68, (20), 2810-2812.
40. Murthy, S. K.; Olsen, B. D.; Gleason, K. K., Initiation of cyclic vinylmethylsiloxane polymerization in a hot-filament chemical vapor deposition process. *Langmuir* **2002,** 18, (16), 6424-6428.
41. Limb, S. J.; Edell, D. J.; Gleason, E. F.; Gleason, K. K., Pulsed plasma-enhanced chemical vapor deposition from hexafluoropropylene oxide: Film composition study. *Journal of Applied Polymer Science* **1998,** 67, (8), 1489-1502.
42. Yasuda, H.; Hsu, T., Some Aspects of Plasma Polymerization Investigated by Pulsed Rf Discharge. *Journal of Polymer Science Part a-Polymer Chemistry* **1977,** 15, (1), 81-97.
43. Yasuda, H., *Plasma Polymerization.* Academic Press: 1985.
44. Gleason, K. K., In 2003; p Personal Communication.
45. Wang, X. Q.; Chen, D. R.; Hian, J. C.; Du, S. Y., Crystallization behavior of polytetrafluoroethylene (PTFE). *Journal of Applied Polymer Science* **2002,** 83, (5), 990-996.
46. Lewis, H. G. P.; Casserly, T. B.; Gleason, K. K., Hot-filament chemical vapor deposition of organosilicon thin films from hexamethylcyclotrisiloxane and octamethylcyclotetrasiloxane. *Journal of the Electrochemical Society* **2001,** 148, (12), F212-F220.
47. Murthy, S. K.; Gleason, K. K., Fluorocarbon-organosilicon copolymer synthesis by hot filament chemical vapor deposition. *Macromolecules* **2002,** 35, (5), 1967-1972.
48. Lewis, H. G. P.; Caulfield, J. A.; Gleason, K. K., Perfluorooctane sulfonyl fluoride as an initiator in hot-filament chemical vapor deposition of fluorocarbon thin films. *Langmuir* **2001,** 17, (24), 7652-7655.
49. Berg, M. C.; Yang, S. Y.; Hammond, P. T.; Rubner, M. F., Controlling mammalian cell interactions on patterned polyelectrolyte multilayer surfaces. *Langmuir* **2004,** 20, (4), 1362-1368.

50. Sardella, E.; Favia, P.; Gristina, R.; Nardulli, M.; d'Agostino, R., Plasma-aided micro- and nanopatterning processes for biomedical applications. *Plasma Processes And Polymers* **2006,** 3, (6-7), 456-469.
51. Alexeev, A.; Verberg, R.; Balazs, A. C., Patterned surfaces segregate compliant microcapsules. *Langmuir* **2007,** 23, (3), 983-987.
52. Lahann, J.; Balcells, M.; Lu, H.; Rodon, T.; Jensen, K. F.; Langer, R., Reactive polymer coatings: A first step toward surface engineering of microfluidic devices. *Analytical Chemistry* **2003,** 75, (9), 2117-2122.
53. Lahann, J.; Balcells, M.; Rodon, T.; Lee, J.; Choi, I. S.; Jensen, K. F.; Langer, R., Reactive polymer coatings: A platform for patterning proteins and mammalian cells onto a broad range of materials. *Langmuir* **2002,** 18, (9), 3632-3638.
54. Lahann, J.; Choi, I. S.; Lee, J.; Jenson, K. F.; Langer, R., A new method toward microengineered surfaces based on reactive coating. *Angewandte Chemie-International Edition* **2001,** 40, (17), 3166-+.
55. James, C. D.; Davis, R.; Meyer, M.; Turner, A.; Turner, S.; Withers, G.; Kam, L.; Banker, G.; Craighead, H.; Isaacson, M.; Turner, J.; Shain, W., Aligned microcontact printing of micrometer-scale poly-L-lysine structures for controlled growth of cultured neurons on planar microelectrode arrays. *Ieee Transactions on Biomedical Engineering* **2000,** 47, (1), 17-21.
56. Cui, X. Y.; Lee, V. A.; Raphael, Y.; Wiler, J. A.; Hetke, J. F.; Anderson, D. J.; Martin, D. C., Surface modification of neural recording electrodes with conducting polymer/biomolecule blends. *Journal of Biomedical Materials Research* **2001,** 56, (2), 261-272.
57. Buchko, C. J.; Kozloff, K. M.; Martin, D. C., Surface characterization of porous, biocompatible protein polymer thin films. *Biomaterials* **2001,** 22, (11), 1289-1300.
58. Ignatius, M. J.; Sawhney, N.; Gupta, A.; Thibadeau, B. M.; Monteiro, O. R.; Brown, I. G., Bioactive surface coatings for nanoscale instruments: Effects on CNS neurons. *Journal of Biomedical Materials Research* **1998,** 40, (2), 264-274.
59. Rousche, P. J.; Pellinen, D. S.; Pivin, D. P.; Williams, J. C.; Vetter, R. J.; Kipke, D. R., Flexible polyimide-based intracortical electrode arrays with bioactive capability. *Ieee Transactions on Biomedical Engineering* **2001,** 48, (3), 361-371.

Chapter Two

Initiated chemical vapor deposition (iCVD) of trivinyl-trimethyl-cyclotrisiloxane for biomaterial coatings*

* Originally published as O'Shaughnessy, W. S.; Gao, M.; Gleason, K. K., Langmuir, 2006, 22 (16), 7021-7026.

2.1 Abstract

Organosilicon polymers show great utility as both biocompatible and electrically insulating materials. In this chapter, thin films of a novel organosilicon polymer are synthesized by initiated CVD utilizing trivinyl-trimethyl cyclotrisiloxane as a monomer and terbutyl peroxide as a free radical generating initiator. Use of an initiator allows for formation of polymer films at filament temperatures as low as 250°C, significantly lower than those required to thermally polymerize the monomer species. The mild reaction conditions allow for retention of all siloxane ring moieties within the resulting polymer. Films deposited at filament temperatures of 600°C or higher exhibit damage to this moiety. The all-dry deposition process generates a highly crosslinked matrix material in which over 95% of the vinyl moieties present on the monomer units have been reacted out to form linear polymerized hydrocarbon chains. While each hydrocarbon backbone chain averages 8.9 monomer units in length, as evaluated by XPS analysis, each monomer unit is involved in three independent chains, resulting in polymer films of such high molecular weight as to be completely insoluble. Kinetic analysis of the deposition process indicates that film formation rate is limited by the adsorption of reactive species to the deposition substrate, with an apparent activation energy of -23.2 kJ/mol with respect to substrate temperature. These results are consistent with a surface growth mechanism, ideal for coating of non-uniform or high aspect ratio substrates.

2.2 Introduction

Organosilicon polymers are of great interest as implantable materials due to their bio-inert nature, flexibility, and hydrophobicity. Poly-dimethyl siloxane (PDMS) is the most widely utilized organosilicon biomaterial, mainly in prosthetic devices[1-3]. Silicone

based polymers have also been studied extensively as surface modifiers for improved haemo-compatibility[4-6]. In addition, organosilicon materials possess favorable properties as electrical insulators. They are widely utilized in the microelectronics industry for their high resistivity and low dielectric constant[7-11].

Chemical vapor deposition (CVD) is an all dry process that can be used to create coatings possessing many desirable characteristics for biomaterial applications[1, 4, 5, 9, 12-15]. CVD coatings can be deposited at nanoscale thicknesses over macroscale areas without pinholes or other defects. They are conformal and do not have the wetting issues associated with surface tension present in solution phase polymer processes[16]. This allows for even coating of implant structures with a high degree of varied dimensionality[15, 17], as well as implants composed of multiple different materials that may not wet uniformly in solution. In addition, there is no issue of solvent entrainment in CVD films and all residual monomer is also removed from the resulting material by vacuum degassing after deposition. Release of entrained solvent and unreacted monomer after implantation is known to be one of the largest sources of polymer implant rejection[1].

Plasma enhanced CVD (PECVD) subjects the precursors to high temperature electrons and the growing film to ion bombardment, typically resulting in damage to any delicate organic moieties present[13, 18-20]. This damage can result in loss of desirable polymer properties. To avoid the use of plasma excitation, an alternative approach known as initiated CVD (iCVD) can be utilized. iCVD employs a radical generating initiator species which is combined with the monomer and fed to the CVD reactor[20-22]. The initiator species possesses a weak, thermally labile bond such as a peroxy or azo linkage. In the iCVD reactor, both species pass over a resistively heated filament array.

The filament temperature is selected so that only the weak initiator bond will be cleaved in order to begin polymerization. The higher thermal stability of the monomer allows its chemical structure to remain unaffected by exposure to the filaments. The result is a dry process polymer synthesis technique much more akin to that of liquid phase polymer synthesis, where the chemical pathways available for reaction are much more tightly controlled.

In this chapter, we have synthesized a novel insulating thin film biomaterial by iCVD. Trivinyl-trimethyl-cyclotrisiloxane (V_3D_3) has been utilized as a monomer and its polymerization initiated by tertbutyl peroxide (TBP). Polymer formation occurs through successive addition across one of three vinyl bonds present in the monomer. Moreover, the trifunctional nature of the V_3D_3 molecule provides for formation of a self crosslinking polymer. When the majority of the vinyl moieties have been reacted, the resulting material is a densely crosslinked network.

2.3 Experimental

2.3.1 Sample Preparation

Material samples were prepared in a custom built vacuum chamber (Sharon Vacuum) as previously described[20-22]. Briefly, the reactor was cylindrical in shape with a diameter of 240 mm and a height of 33 mm. The top of the reactor consisted of a 25mm thick quartz plate, allowing for observation of the sample throughout deposition.

Liquid monomer (1,3,5 trivinyl-trimethyl-cyclotrisiloxane, 99% Gelest) and initiator (tertbutyl peroxide, 98% Aldrich) were utilized without further purification. The monomer was vaporized in a Pyrex^{tm} crucible maintained at 70 ± 2 °C and vapor flow

metered to the reactor through a mass flow controller (Model 1153, MKS). The initiator was placed in a sealed Pyrex^{tm} container at room temperature and vapors fed to the reactor through a second mass flow controller (Model 1179A, MKS). Precursor gases were premixed and fed through a port in the side of the reactor cylinder. They then passed through a distribution plate to ensure uniform flow over the deposition area.

The initiator was broken down to radical species by a resistively heated filament array suspended 20 mm above the substrate. Filament temperature was measured by a thermocouple (Type K, AWG 36, Omega Engineering) directly attached to one of the filament wires. Pressure within the chamber was measured by a capacitance diaphragm gauge and controlled through use of a throttling butterfly valve (Intellisys, NorCal) connected to an auto-tuned digital controller (Intellisys, NorCal).

All prepared samples were deposited on 100mm diameter IR transparent silicon wafers (WaferWorld). Substrate temperature was maintained with an accuracy of ± 2 °C throughout the deposition by circulation of heated silicon oil on the backside of the reactor stage. Film growth was observed *in situ* through interferometry and controlled to thicknesses of 250-500 nm. A 633 nm laser source (JDS Uniphase) was utilized and its reflectance measured by a Metrologic detector.

Table 2-1, below, shows reactor conditions for all iCVD film samples analyzed in this paper.

Sample Name	Pressure (mTorr)	Stage Temperature (Kelvin)	Filament Temperature (Kelvin)	Monomer Flowrate (sccm)	Initiator Flowrate (sccm)
A1	450	333	473	9	1
A2	450	333	523	9	1
A3	450	333	573	9	1
A4	450	333	623	9	1
A5	450	333	673	9	1
A6	450	333	723	9	1
A7	450	333	773	9	1
A8	450	333	873	9	1
A9	450	333	1073	9	1
A10	450	333	1273	9	1
B1	400	323	773	5	1
B2	400	333	773	5	1
B3	400	343	773	5	1
B4	400	353	773	5	1
B5	400	363	773	5	1
B6	400	373	773	5	1

Table 2-1. Reactor conditions for deposition of iCVD polymer films

2.3.2 Material Characterization

Sample thickness (250 – 500 nm) was measured through the use of a variable angle spectroscopic ellipsometer (J.A. Woollam M-2000, xenon light source). A

Cauchy-Urbach model was utilized to obtain a non-linear least squares fit of data obtained at either one (70°) or three (65°, 70°, 75°) angles and 225 wavelengths.

Fourier transform infrared spectroscopy (FTIR) was performed on a Nicolet Nexus 870 ESP spectrometer in normal transmission mode. A DTGS KBr detector was utilized over the range of 400 to 4000 cm^{-1} with a 4 cm^{-1} resolution. Measurements were averaged over either 64 or 128 scans. All samples were baseline corrected and thickness normalized to allow for accurate comparison. A comparison spectrum of the monomer species was obtained from NIST Standard Reference Database 69 [23]. X-ray photoelectron spectroscopy (XPS) was performed using a Kratos Axis Ultra spectrometer with a monocromatized Al Kα source. XPS analysis was performed on samples greater than one week in age.

2.4 Results and Discussion

2.4.1 FTIR and XPS

Figure 2-1 shows a comparison of the FTIR spectrum of the V_3D_3 monomer[23] with that of CVD film A2 in Table 1. The spectrum of CVD film A2 is representative of the spectra of all films deposited at filament temperatures below 500 °C, as will be discussed below. Table 2-2 shows a list of FTIR absorption assignments associated with the V_3D_3 monomer as have been previously reported[24]. Note that each bond type in the monomer produces at least one identifying FTIR absorption. In addition, the strong Si-O absorption which appears at 1012 cm^{-1} is characteristic of a ring containing three Si-O repeat units; Si-O bonds in linear chains are known to absorb at ~15 to 30 cm^{-1} higher[25].

Also, note that all C-H bond absorptions at wavenumbers greater than 3000 cm^{-1} are associated with hydrogen atoms bonded to unsaturated carbon atoms.

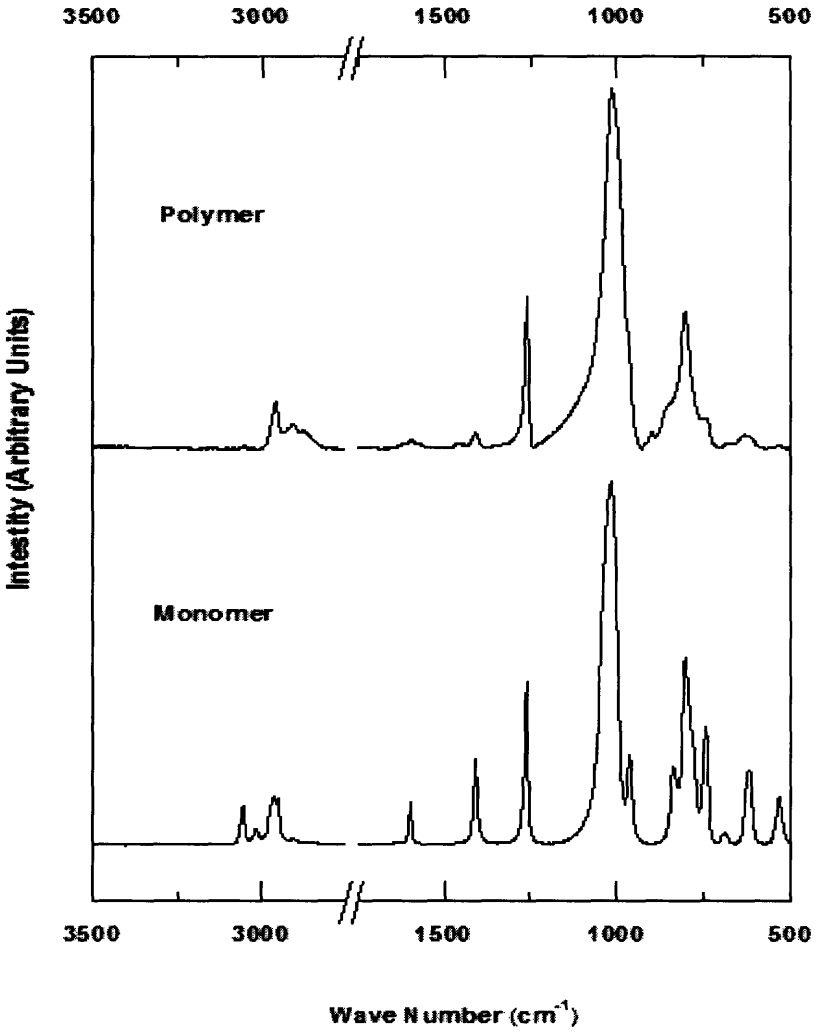

Figure 2-1. FTIR Spectra of the V_3D_3 monomer and the resulting polymer. Note the presence of the 1012cm^{-1} peak in both spectra corresponding to the Si-O ring moiety.

Group	iCVD Film (cm^{-1})	Literature[25] (cm^{-1})	Strength
Si-O-Si Stretch (Trisiloxane Rings)	1012	1010-1020	Very Strong
Si-CH_3 Symmetric Stretch	1261	1255-1280	Strong
Si-CH_2 Deformation	1408	1390-1410	Medium
Si-CH_3 Anti-Symmetric Stretch	1408	~1410	Medium
C=C Stretch of vinyl bond	1597	1590-1615	Medium
CH_3 Anti-Symmetric Stretch	2964	2965-2969	Strong
CH Stretch of vinyl bond	3016	2995-3020	Medium
CH_2 Anti-symmetric Stretch of vinyl bond	3057	3075-3090	Medium

Table 2-2. FTIR Absorption Assignments for the V_3D_3 Monomer

The FTIR spectrum of the iCVD film shown in Figure 2-1 is largely similar to that of the monomer, but with a few key differences. The spectrum contains a strong absorption at 1012 cm^{-1}, nearly identical to that present in the monomer spectra. This absorption indicates that the Si-O ring structure present in the monomer has been retained. Were the ring opened during the polymerization there would be a reduction in peak intensity coupled with the appearance of a secondary Si-O peak between 1050-1100 cm^{-1} corresponding to the presence of linear Si-O chains in the deposited material.

Indeed, polymerization of the V_3D_3 monomer at a filament temperature above 500 °C results in the formation of linear Si-O chains. Figure 2-2, which shows an enlargement of the 975–1125 cm^{-1} section of the IR spectra of iCVD films A5, A8, A9, & A10, demonstrates this result. As the filament temperature increases, so does the intensity of the absorption at 1080 cm^{-1} associated with the linear Si-O chains. An associated decrease in absorption intensity of the 1012 cm^{-1} Si-O peak occurs simultaneously, indicating that the Si-O ring groups are being converted to Si-O linear chains. These linear chains are not observed in films deposited at filament temperatures below 600 °C, indicating that ring opening is not occurring in this low filament temperature range.

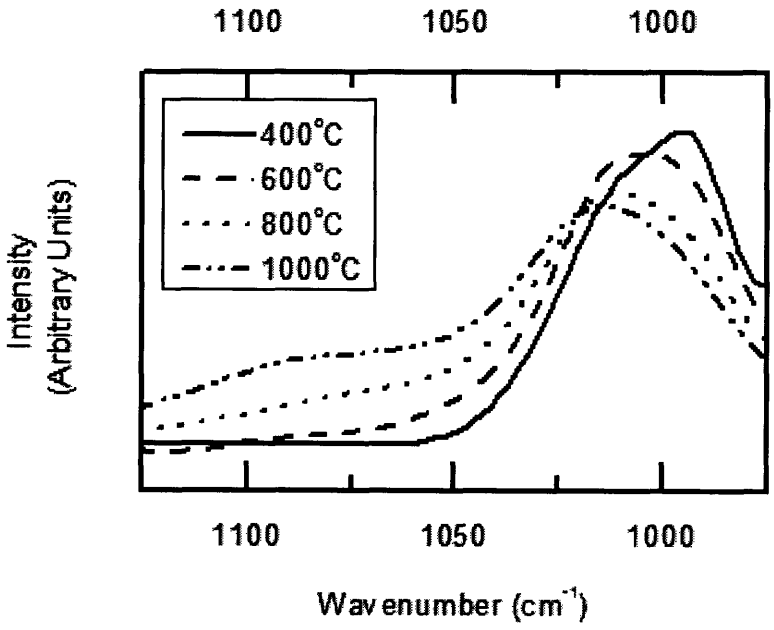

Figure 2-2. FTIR Spectra of iCVD films deposited at varying filament temperatures (1150 – 900cm^{-1}). Note that as filament temperature increases, the intensity of the 1012cm^{-1} peak, associated witht eh Si-O ring moiety, decreases. There is also an associated increase in absorption at 1080cm^{-1} corresponding to the formation of linear Si-O chains.

At filament temperatures of 600°C and over, film deposition will occur without the use of a radical initiator. Deposition will not occur without the addition of a radical initiator below a filament temperature of 600 °C. As the lower temperature films have neither linear Si-O chains, nor will they deposit without an initiator, it can be concluded that polymerization in these films is not taking place through thermal ring opening.

Figure 2-3 displays an enlargement of the 1200-1650 cm^{-1} section of both the monomer and polymer FTIR spectra. While the peak at 1261 cm^{-1} associated with the Si-methyl bond is unchanged, the two absorptions at 1597 and 1408 cm^{-1} are significantly reduced. In the case of the 1597 cm^{-1} peak, less than 5% of the absorption intensity remains. The persistence of a small peak at 1408 cm^{-1} is due to the deformation of the methylene unit bonded to a silicon atom. This absorption is much weaker in intensity than that of the CH_2 deformation of the vinyl moiety. The loss of the CH_2 deformation and C=C stretching peaks indicates that the vinyl moiety present in the monomer is almost entirely absent in the iCVD film.

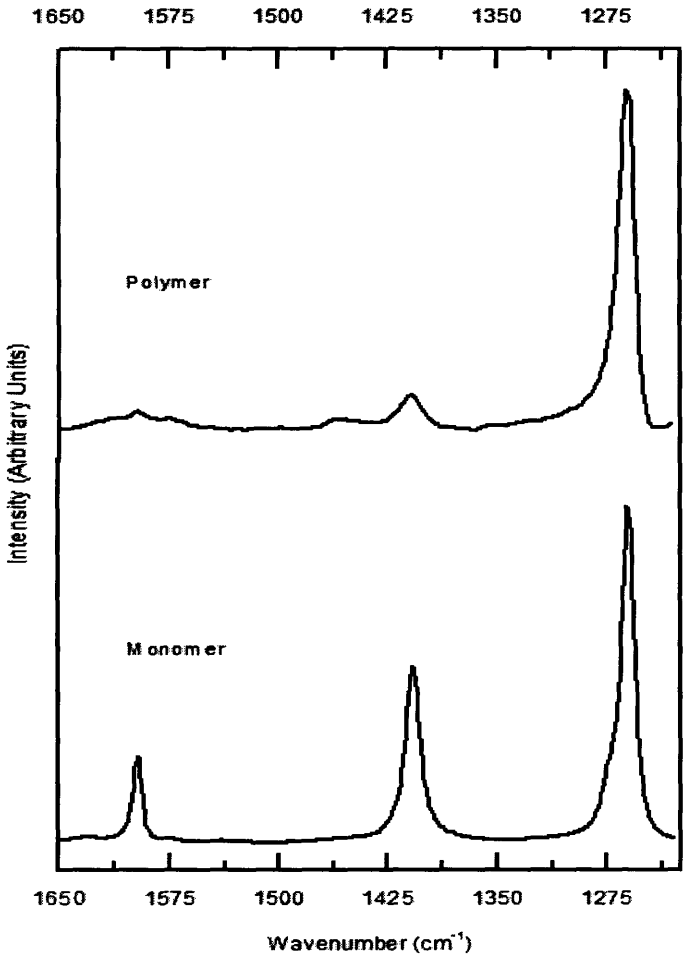

Figure 2-3. Enlargement of the 1650 – 1225 cm^{-1} section of the FTIR Spectra of V_3D_3 Monomer and Polymer. Note that in the polymer spectra, absorptions associated with the vinyl moiety are significantly reduced while those associate with the methyl moiety remain unchanged.

Further evidence of the absence of vinyl moieties in the polymer structure is available upon examination of the C-H bond absorption region (2800-3200 cm^{-1}). An enlargement of this region is shown in Figure 2-4. Absorptions associated with C-H bonds on unsaturated carbons (those at 3057, 3016, and 2953 cm^{-1}) are significantly reduced in the polymer spectrum. This reduction is accompanied by an increase in absorption intensity below 3000 cm^{-1}. This indicates that the unsaturated carbons in the

vinyl moieties have become saturated, shifting the wavenumbers at which their associated carbon hydrogen bonds absorb. Once again, the absorption associated with the methyl moiety, the C-H anti-symmetric stretch at 2964 cm^{-1}, is unaffected by the polymerization.

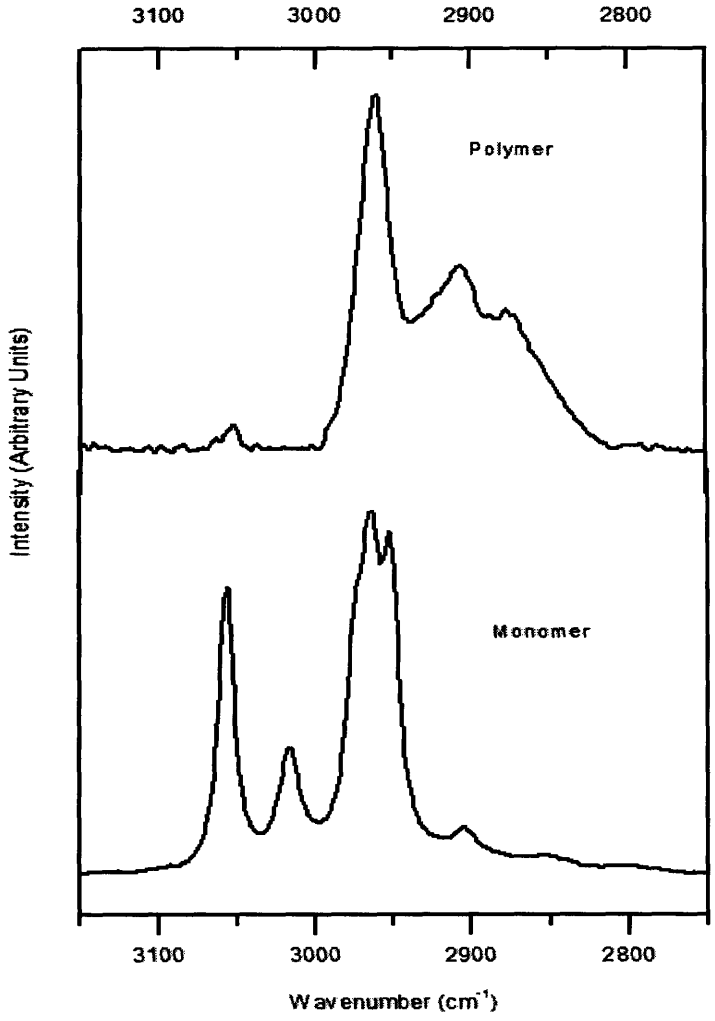

Figure 2-4. Enlargement of the 3150 – 2750 cm-^{1} section of the FTIR Spectra of V_3D_3 Monomer and Polymer (C-H absorption region).

Table 2-3 shows the atomic ratios of carbon, silicon, and hydrogen present in iCVD film "C" as calculated from the XPS spectrum of the material. It should be noted

that the ratio of 3.9 : 1 carbon to silicon is much higher than the 3.0 : 1 ratio present in the pure monomer.

Element	Atomic Percentage
Carbon	60.6%
Oxygen	23.8%
Silicon	15.6%

Table 2-3. Elemental ratios present in polymer film as measured by XPS of sample A7.

2.4.2 Polymerization Mechanism

This spectroscopic evidence supports the conclusion that polymerization has taken place by reaction of the vinyl bonds present in the monomer to form saturated linear carbon chains. A schematic depiction of this polymerization mechanism is presented in Figure 2-5. Note that while Figure 2-5 depicts the formation of only a single linear chain (for clarity in depicting the reaction), identical polymerization steps are taking place from all three vinyl units on each monomer molecule to form a densely cross-linked material. The final polymer product is a three dimensional matrix as depicted schematically in Figure 2-6.

Step 1: Radical Formation

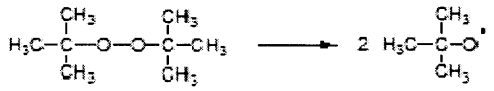

Step 2: Chain Initiation

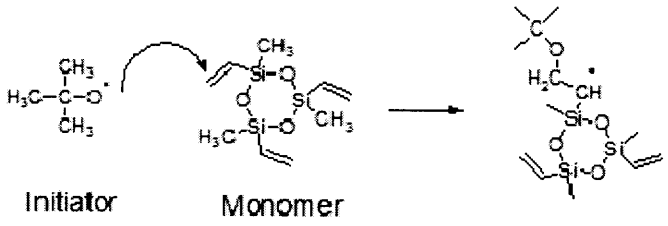

Step 3: Chain Propagation

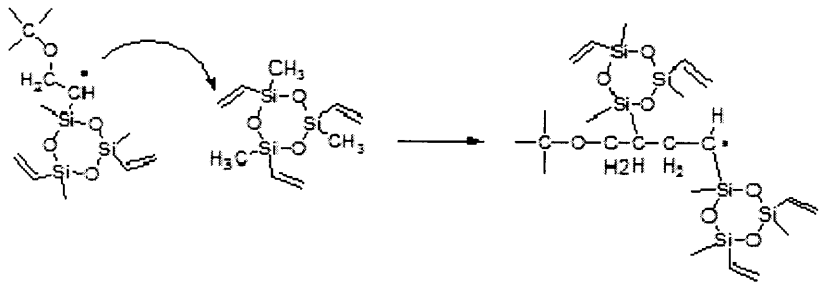

Step 4: Chain Termination

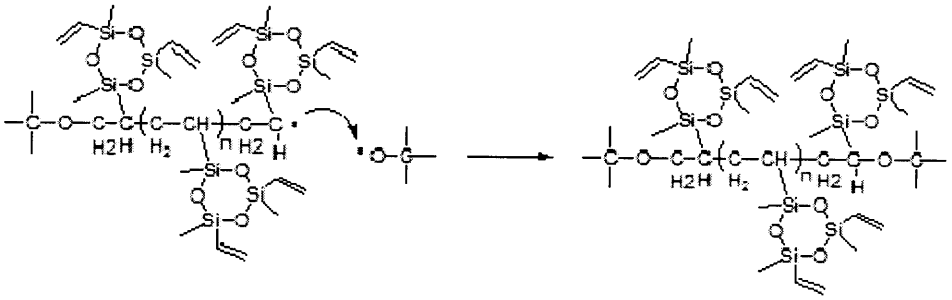

Figure 2-5. Proposed polymerization mechanism. Main chain in final polymer between the oxygen atoms comprises a "carbon chain segment" as described in section 2.4.2

Previous work on iCVD has demonstrated the formation of radical species from thermal cracking of a vapor phase peroxide initiator at filament temperatures greater than 200 °C as shown in Step 1[20, 21]. These radicals then react with the vinyl moieties on the V_3D_3 monomer to initiate polymerization as shown in Step 2. As stated above, it should be noted that while Figure 5 depicts only one vinyl moiety reacting (for clarity), all three vinyl moieties present on the monomer react similarly. Polymerization then progresses through addition of a secondary carbon radical to unreacted vinyl bonds on other monomer units as shown in Step 3. Termination of the polymerization can occur due to reaction of two growing chains or through end capping with another peroxide radical fragment[26] (as shown in Step 4). In this system, we hypothesize the latter is the dominant mechanism due to steric constraints associated with the size of the V_3D_3 monomer unit. Involvement of each monomer unit in multiple polymer chains further constrains chain mobility and is likely to produce additional steric hindrance to subsequent reaction steps. Consideration of this factor in constraining growing chain movement further favors a radical end capping termination mechanism as opposed to termination by the combination of two sterically hindered chains.

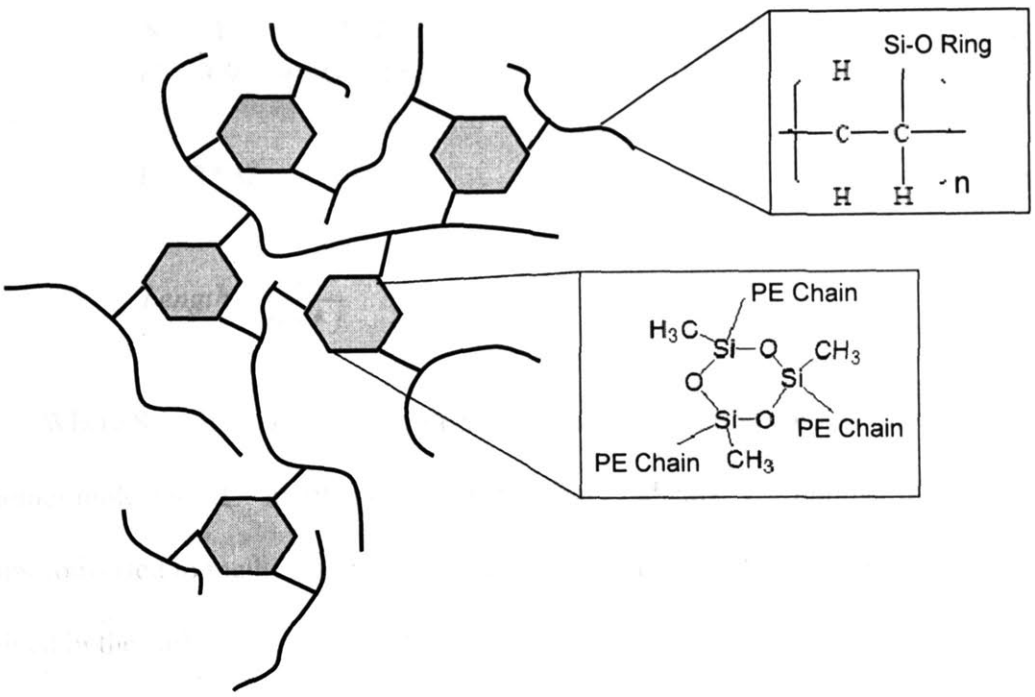

Figure 2-6. Schematic representation of the matrix structure of the final polymer film. The hexagonal units represent the intact siloxane rings which act as crosslinking moieties for multiple carbon backbone chains.

2.4.3 Segmental Chain Length

Due to this densely crosslink structure, the resulting polymer film is insoluble in typical solvents (e.g., acetone, THF, and DMSO) and traditional methods for determining molecular weight or chain length, such as gel permeation chromatography, cannot be utilized. However, an estimate of how many monomer units comprise an average carbon chain segment within the polymer (see Figure 2-5) can be made from the spectroscopic evidence. The XPS data shows a ratio of 3.9 : 1 of carbon to silicon in the iCVD film. Assuming that the additional carbon present in the polymer is due to incorporation of peroxide radical fragments, Equations 2-1, 2-2, & 2-3 below can be solved in order to estimate the average length of the carbon backbone chains.

$$\frac{S}{C} = \frac{1}{3.9} = \frac{3*M}{9*M+4*I} \tag{2-1}$$

$$V = 3*M \tag{2-2}$$

$$Length = \frac{V}{0.5*I} \tag{2-3}$$

Where S = number of silicon atom, C = number of carbon atoms, M = number of monomer molecules, I = number of initiator primary radicals, V = number of vinyl groups converted to methylene bridges, and Length is the number of monomer units involved in the carbon chain. In addition, equation 2-3 assumes that all vinyl moieties are reacted out of the resulting film. This assumption is supported by the IR spectra in both the Si-C and C-H regions as described above. The factor of 0.5 is included as it is assumed two I fragments will be required per chain (one to initiate and one to terminate).

Using the XPS data from sample A7, average chain length is calculated to be 8.9 units. This represents a lower bound on chain length as some fraction of the carbon content present in the XPS spectrum could be due to sample contamination. In addition, ~5% of the vinyl moieties present on the involved monomer units remain unreacted. The presence of these groups will also serve to increase slightly the average chain length from the 8.9 units. It should also be noted that some small fraction of the initiating species could be methyl radicals formed through the beta-scission of the peroxide radical fragments[27]. This would alter the form of Equation 2-1 and could reduce the average chain length. However, this reaction is energetically unfavorable due to the instability of the methyl radical product and has been observed to be significantly slower than beta-scission reactions of related peroxides such as tertamyl peroxide[28]. These factors,

combined with the linear flow design of the reactor to prevent recirculation, make it unlikely that methyl radicals play a significant role in initiation and termination of the polymer chains.

2.4.4 Reaction Kinetics

Figure 2-7 shows a log scale plot of the deposition rate versus inverse filament temperature of the deposition. The reaction conditions for these depositions correspond to samples A1-A7 in Table 2-1. Two distinct regimes of deposition can be observed in this data. At filament temperatures of 200-400 °C (the right portion of the graph), the deposition process is much more sensitive to increases in temperature. Above 400 °C, the deposition rate begins to flatten out, indicating a transition from a regime in which a gas phase reaction near the filament wires plays some role to one that is mass transport limited. This mass transport limitation is most likely not occurring in the gas phase as the deposition rate is still only 18 nm/min. Instead, as is observed in parylene deposition, this limitation is most likely occurring on the substrate and is due to diffusion of monomer and initiator within the deposited polymer matrix[29, 30].

The style of plot shown in Figure 2-7 is commonly used to calculate the activation energy of deposition by fitting the data to the Arrhenius equation[31]. However, for this analysis to be valid, the change in deposition rate must be a function only of the change in rate constant, not of reactant concentrations[20, 24]. For the current system, the gas phase concentrations of both species will vary significantly with filament temperature due to gas expansion, especially in the region very near the filament wires. As these concentrations will affect the deposition rate, the calculated activation energy can not be attributed entirely to the kinetic rate constant and must instead be viewed as the overall

outcome of two competing processes. With this caveat, an apparent activation energy for the process as a whole can still be calculated. A least squares fit of the linear portion of this plot gives a value of -3365 for the slope, corresponding to an apparent activation energy of 28.0 kJ/mol for the polymerization process with respect to filament temperature. The relatively low value of the activation energy versus the 108 kJ/mol bond energy[20] of the O-O bond in the peroxide indicates that the formation of radicals in the gas phase is not likely the rate limiting step in this polymerization. Instead, the polymerization rate is much more likely to be dominated by the propagation reaction as the size and geometry of the monomer molecules create significant steric barriers to the reaction.

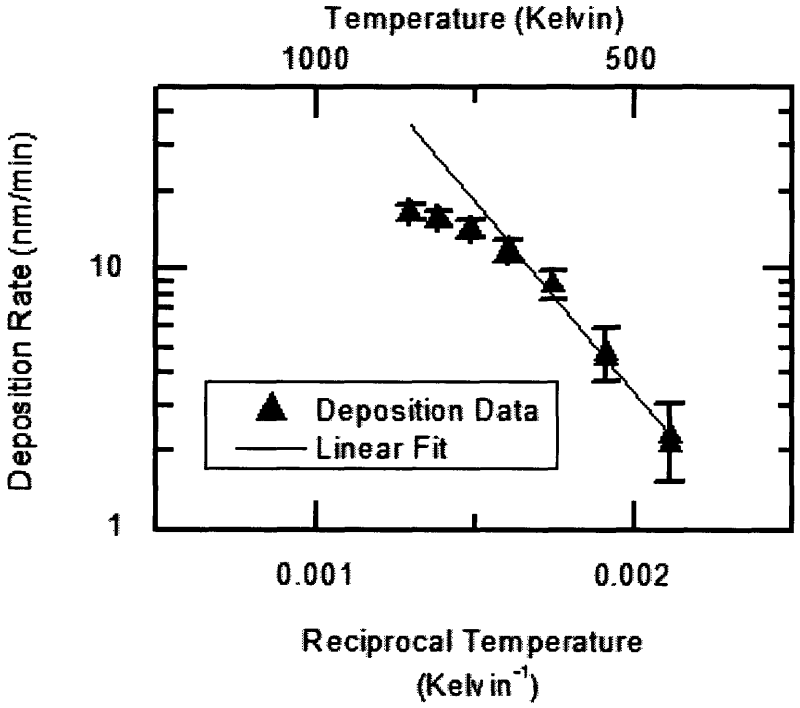

Figure 2-7. Deposition rate data for polymer growth as a function of filament temperature (CVD films A1-A7)

Figure 2-8 shows a log scale plot of deposition rate versus reciprocal substrate temperature. The reaction conditions for these depositions correspond to samples B1-B6 in Table 2-1. As above, an apparent activation energy of the deposition process with respect to this temperature change can be calculated, with the same caveats. This apparent activation energy is calculated to be -23.2 kJ/mol. Increasing the stage temperature creates both an increase in propagation rate on the surface and a decrease in the equilibrium concentration of absorbed species on the substrate. The negative apparent activation energy indicates that the decrease in the surface concentration of reactive species dominates over the increase in reaction rate constant, but it is not possible to quantitatively separate the two effects.

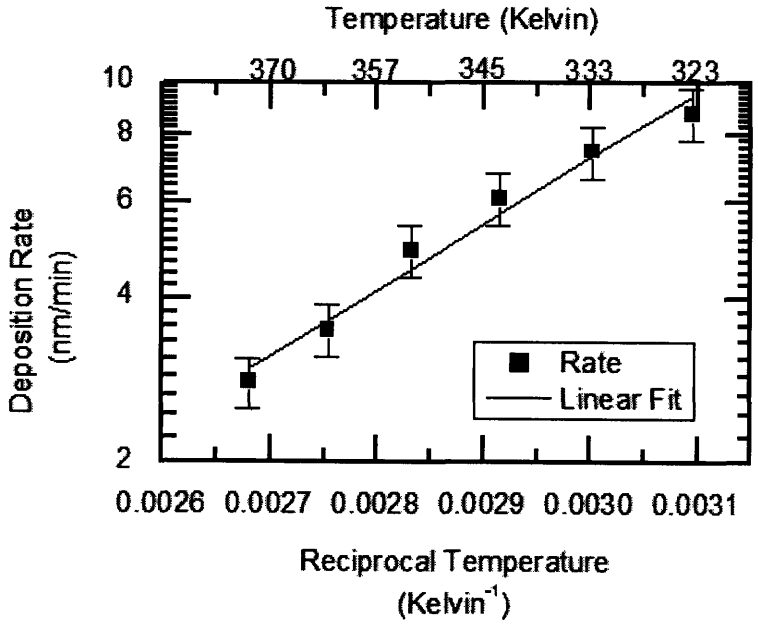

Figure 2-8. Deposition Rate data for polymer film growth as a function of substrate temperature (CVD films B1-B6)

2.5 Conclusions

In this chapter, we have demonstrated the synthesis of a novel thin film material by iCVD. The all dry deposition process forms a self crosslinking polymer matrix from the V_3D_3 monomer. The use of tertbutyl peroxide as a gas phase radical generating species allows for formation of polymeric material at filament temperatures as low as 250°C, over 300°C lower than required for polymerization of V_3D_3 without the use of an initiator. FTIR analysis demonstrates the retention of all siloxane ring moieties (1092 cm^{-1}) within the low filament temperature films, a result not possible with PECVD[15] or at the higher filament temperatures required for deposition without an initiator.

Further spectroscopic analysis demonstrates that more than 95% of the vinyl moieties present on the monomer units have reacted out of the film to form linear hydrocarbon chains. These chains individually average only 8.9 monomer units in length, as estimated from XPS elemental analysis. This short chain length is likely driven by steric inhibition of a large monomer unit adding to the growing chain during the propagation reaction. However, the involvement of each monomer unit in three separate chains provides for complete insolubility in the resulting films, indicating very high total molecular weight.

Kinetic analysis indicates that the deposition process is adsorption limited, most likely with respect to monomer surface concentration[32]. This result supports the hypothesis that the polymerization is taking place on the substrate itself, as opposed to growth of polymer chains in the gas phase with subsequent deposition, making the described synthetic approach ideal of coating of non-uniform substrates or substrates possessing a high degree of dimensionality.

Future work with this novel polymer will focus of evaluation of its material and electrical properties. The polymer will also be evaluated for use in implantable electronics through long term stability testing in a biological environment. Surface functionalization of the thin films will also be examined to maximize biocompatibility.

2.6 Acknowledgement

The authors acknowledge the support of both the NIH, under funding contract #NO1-NS2-2347, and NSF/SRC Engineering Research Center for Environmentally Benign Semiconductor Manufacturing. This work also made use of MRSEC Shared Facilities supported by NSF grant #DMR-9400334.

2.7 References

1. Bhat, S. V., *Biomaterials*. First ed.; Narosa Publishing House: New Delhi, India, 2002.
2. L. L. Hench, E. C. E., *Biomaterials: An Interfacial Approach*. First ed.; Academic Press: 1982.
3. Belanger, M. C.; Marois, Y., Hemocompatibility, biocompatibility, inflammatory and in vivo studies of primary reference materials low-density polyethylene and polydimethylsiloxane: A review. *Journal Of Biomedical Materials Research* **2001,** 58, (5), 467-477.
4. Chawla, A. S., Evaluation of Plasma Polymerized Hexamethylcyclotrisiloxane Biomaterials Towards Adhesion of Canine Platelets and Leukocytes. *Biomaterials* **1981,** 2, (2), 83-88.
5. Chu, P. K.; Chen, J. Y.; Wang, L. P.; Huang, N., Plasma-surface modification of biomaterials. *Materials Science & Engineering R-Reports* **2002,** 36, (5-6), 143-206.
6. Ishikawa, Y.; Sasakawa, S.; Takase, M.; Iriyama, Y.; Osada, Y., Interaction of Plasma-Polymerized Poly(Organosiloxane) Films with Platelets. *Makromolekulare Chemie-Rapid Communications* **1985,** 6, (7), 495-502.
7. Casserly, T. B.; Gleason, K. K., Chemical vapor deposition of organosilicon thin films from methylmethoxysilanes. *Plasma Processes And Polymers* **2005,** 2, (9), 679-687.
8. Furusawa, T.; Ryuzaki, D.; Yoneyama, R.; Homma, Y.; Hinode, K., Heat and moisture resistance of siloxane-based low-dielectric-constant materials. *Journal Of The Electrochemical Society* **2001,** 148, (9), F175-F179.

9. Lewis, H. G. P.; Casserly, T. B.; Gleason, K. K., Hot-filament chemical vapor deposition of organosilicon thin films from hexamethylcyclotrisiloxane and octamethylcyclotetrasiloxane. *Journal of the Electrochemical Society* **2001,** 148, (12), F212-F220.
10. Wu, Q. G.; Gleason, K. K., Plasma-enhanced chemical vapor deposition of low-k dielectric films using methylsilane, dimethylsilane, and trimethylsilane precursors. *Journal Of Vacuum Science & Technology A* **2003,** 21, (2), 388-393.
11. Wu, Q. G.; Gleason, K. K., Plasma-enhanced CVD of organosilicate glass (OSG) films deposited from octamethyltrisiloxane, bis(trimethylsiloxy) methylsilane, and 1,1,3,3-tetramethyldisiloxane. *Plasmas And Polymers* **2003,** 8, (1), 31-41.
12. Ratnr, B. D.; Johnston, A. B.; Lenk, T. J., Biomaterial Surfaces. *Journal of Biomedical Materials Research-Applied Biomaterials* **1987,** 21, (A1), 59-89.
13. Yasuda, H., *Plasma Polymerization.* Academic Press: 1985.
14. Favia, P.; d'Agostino, R., Plasma treatments and plasma deposition of polymers for biomedical applications. *Surface & Coatings Technology* **1998,** 98, (1-3), 1102-1106.
15. Lewis, H. G. P.; Edell, D. J.; Gleason, K. K., Pulsed-PECVD films from hexamethylcyclotrisiloxane for use as insulating biomaterials. *Chemistry of Materials* **2000,** 12, (11), 3488-3494.
16. Pierson, H. O., *Handbook of Chemical Vapor Deposition.* 2nd ed.; William Andrew Publishing: Norwich, N.Y., 1999.
17. Limb, S. J.; Gleason, K. K.; Edell, D. J.; Gleason, E. F., Flexible fluorocarbon wire coatings by pulsed plasma enhanced chemical vapor deposition. *Journal of Vacuum Science & Technology a-Vacuum Surfaces and Films* **1997,** 15, (4), 1814-1818.
18. Yasuda, H.; Hsu, T., Some Aspects of Plasma Polymerization Investigated by Pulsed Rf Discharge. *Journal of Polymer Science Part a-Polymer Chemistry* **1977,** 15, (1), 81-97.
19. K. K. S. Lau, K. K. G., Pulsed plasma enhanced and hot filament chemical vapor deposition of fluorocarbon films. *Journal Of Fluorine Chemistry* **2000,** 104, (1), 119-126.
20. Mao, Y.; Gleason, K. K., Hot filament chemical vapor deposition of poly(glycidyl methacrylate) thin films using tert-butyl peroxide as an initiator. *Langmuir* **2004,** 20, (6), 2484-2488.
21. Chan, K.; Gleason, K. K., Initiated CVD of poly(methyl methacrylate) thin films. *Chemical Vapor Deposition* **2005,** 11, (10), 437-443.
22. Chan, K.; Gleason, K. K., Initiated chemical vapor deposition of linear and cross-linked poly(2-hydroxyethyl methacrylate) for use as thin-film hydrogels. *Langmuir* **2005,** 21, (19), 8930-8939.
23. Coblentz_Society, *NIST Chemistry Webbook.* 2005.
24. Murthy, S. K.; Olsen, B. D.; Gleason, K. K., Initiation of cyclic vinylmethylsiloxane polymerization in a hot-filament chemical vapor deposition process. *Langmuir* **2002,** 18, (16), 6424-6428.
25. D. Lin-Vien, N. C., W. Fately, J. Grasselli, *The Handbook of Infrared and Ramman Characteristic Frequencies of Organic Molecules.* Academic Press: San Diego, 1991.

26. Odian, G. G., *Principles of Polymerization*. 3rd ed.; Wiley: New York, 1991.
27. Mekarbane, P. G.; Tabner, B. J., Interaction between radicals derived from two di-t-alkyl peroxides with some monomers and polymers. *Macromolecules* **1999,** 32, (11), 3620-3625.
28. Ma, R.; Bakac, A.; Espenson, J. H., Kinetics Of Oxidation Of Vanadium(Iv) By Alkyl Hydroperoxides In Acidic, Aqueous-Solution. *Inorganic Chemistry* **1992,** 31, (10), 1925-1930.
29. Rogojevic, S.; Moore, J. A.; Gill, W. N., Modeling vapor deposition of low-K polymers: Parylene and polynaphthalene. *Journal Of Vacuum Science & Technology A* **1999,** 17, (1), 266-274.
30. Ganguli, S.; Agrawal, H.; Wang, B.; McDonald, J. F.; Lu, T. M.; Yang, G. R.; Gill, W. N., Improved growth and thermal stability of Parylene films. *Journal Of Vacuum Science & Technology A-Vacuum Surfaces And Films* **1997,** 15, (6), 3138-3142.
31. Fogler, H. S., *Elements of Chemical reaction Engineering*. 3rd ed.; Prentice Hall: Upper Saddle River, 1999.
32. K. K. S. Lau, K. K. G., Initiated Chemical Vapor Deposition (iCVD) of Poly(alkyl acrelates): A Mechainistic Study. *Macromolecules* **Accepted 2006**.

Chapter Three

Stable Biopassive Insulation Synthesized by initiated Chemical Vapor Deposition (iCVD) of poly(1,3,5-Trivinyltrimethylcyclotrisiloxane)*

* Originally published as O'Shaughnessy, W. S.; Murthy, S. K..; Edell, D. J.; Gleason, K. K., Biomacromolecules, 2007, In Press.

3.1 Abstract

The permanent implantation of electronic probes capable of recording of neural activity patterns requires long term electrical insulation of these devices by biopassive coatings. In this chapter, the material properties and neural cell compatibility of a novel polymeric material, poly(trivinyltrimethylcyclotrisiloxane) (poly(V_3D_3)) are demonstrated to be suitable for application as permanently bio-implanted electrically insulating films. The poly(V_3D_3) polymeric films are synthesized by initiated chemical vapor deposition (iCVD), allowing for conformal and flexible encapsulation of fine wires. The poly(V_3D_3) also exhibits high adhesive strength to silicon substrates, a common material of manufacture for neural probes. The poly(V_3D_3) films were found to be insoluble in both polar and nonpolar solvents, consistant with their highly crosslinked structure. The films are pin-hole free and extremely smooth, having an RMS roughness of 0.4 nm. The material possesses a bulk resistivity of 4×10^{15} Ohm-cm exceeding that of Parylene-C, the material currently used to insulate neurally implanted devices. The iCVD poly(V_3D_3) films are hydrolytically stable and are demonstrated to maintain their electrical properties under physiological soak conditions, and constant electrical bias, for more than two years. In addition, biocompatibility studies with PC12 neurons demonstrate that this material is non-cytotoxic and does not influence cell proliferation.

3.2 Introduction

The field of neuroprosthetics utilizes the firing patterns of individual neurons to control electronic devices external to the subject. Recent advances in this field, including a human implant trial[1, 2], have brought the possibility of therapeutic implementation into

the near term. However, one major barrier to clinical use remains the long term stability of the neural arrays within the brain[3-11]. Of paramount importance to this stability is the electrically insulating coating placed on the device prior to implantation. Each neural array consists of 10-100 neural probe shanks, each 25-50 μm in diameter but millimeters in length[12-16]. These high aspect ratio features makes the application of a smooth, even coating a significant challenge. In addition, the coating must be highly electrically resistive to insulate the implant with as little increase in the diameter of the probe shanks as possible. The coating must be conformal and adherent to the device for corrosion prevention over the 20+ year implant design life. The coating properties must also be retained within the implantation environment while not inducing a negative biological response[17]. The material should possess some mechanical flexibility so that both the probe array and its lead wires can be concurrently insulated to maximize device reliability. For concurrent insulation, the coating material must adhere to both probe substrate materials, such as silicon, and metallization materials, such as gold and copper.

While there are many different methodologies available for the application of insulating biomaterial coatings, the above requirements make chemical vapor deposition (CVD) an ideal approach[18-24]. CVD is a coating process which is known to produce conformal, pinhole free films of controllable thickness on 3-D substrates[19, 25, 26]. As CVD is an all dry process, coating problems associated with non-uniform wetting due to surface tension effects, which can be exacerbated on high aspect ratio substrates, are avoided[27]. In addition, there is no issue of entrained solvent in the coating, a significant cause of polymer implant rejection[17]. In order to exploit the advantages of vapor deposition while not sacrificing control over polymer chemistry, initiated CVD (iCVD)

can be utilized. The iCVD method employs a free radical generating initiator to begin vapor phase polymerization of a vinyl monomer under much more benign conditions than pulsed plasma, thermal, or traditional hot filament CVD[28-32]. This allows for both a high degree of control over polymer chemistry, as with solution phase polymer synthesis, and the retention of sensitive functional groups within the resulting films not possible through traditional CVD methods[30, 33]. In addition, copolymer films and films of graded composition can be created through iCVD, allowing for independent optimization of the bulk and surface properties of deposited coatings.

In this chapter the material properties, biocompatibility, and long term stability of poly(1,3,5-trivinyltrimethylcyclotrisiolxane), poly(V_3D_3), are evaluated. This material has been developed as an iCVD synthesized polymer for the insulation of neural recording arrays. While the polymerization mechanism and molecular structure of poly(V_3D_3) have been previously described in detail[33], it should be noted that the creation of thin films of this polymer is not possible by techniques other than iCVD due to both solubility and steric considerations. Its structure is composed of carbon backbone chains joined together by siloxane rings as shown schematically in Figure 3-1. The density of crosslinking within this material combined with the retention of siloxane ring moieties present in the monomer prevents the formation of this molecular structure through either solution phase polymerization or non-initiated CVD. It should be noted that the polymer structure has structural features of both polyethylene (PE), in the long backbone chains, and of a polysiloxane in the crosslinking rings. As such, it is likely to behave as a copolymer of these two well characterized biomaterials, inspiring its use for this application. Siloxane bonds are noted for their flexibility. Hence, incorporation of

siloxane rings may avoid brittle failure even in films which are highly crosslinked. Additionally, the siloxane rings are likely to inhibit the formation of PE crystallites.

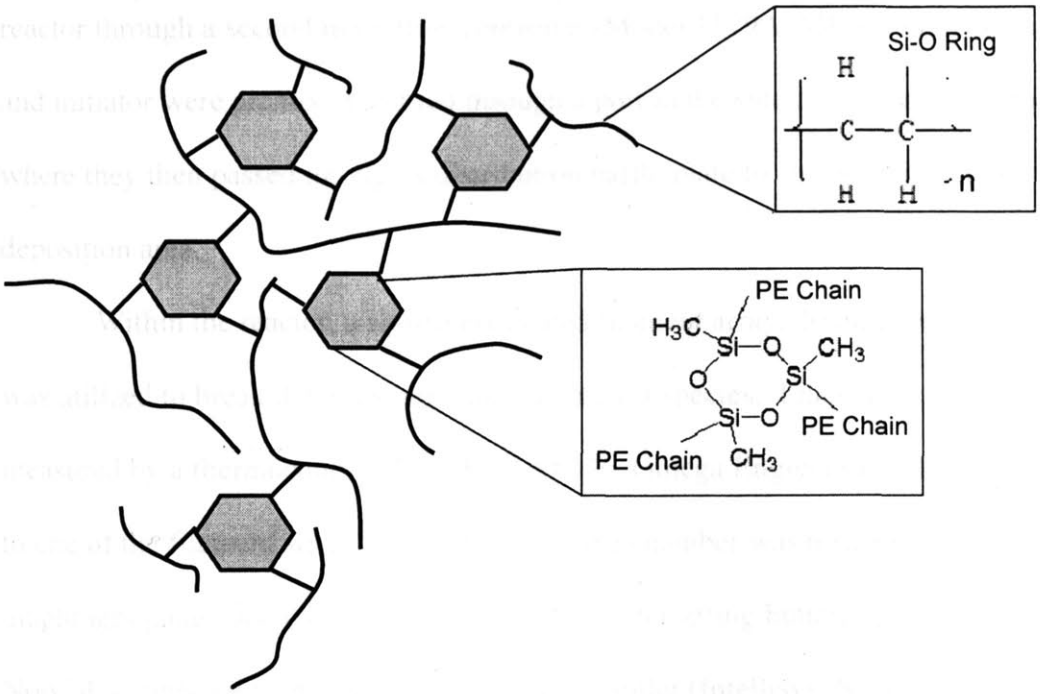

Figure 3-1. Schematic representation of the matrix structure of the final polymer film. The hexagonal units represent the intact siloxane rings which act as crosslinking moieties for multiple carbon backbone chains.[33]

3.3 Experimental

3.3.1 Sample Preparation

Polymer depositions were preformed in a custom built vacuum chamber (Sharon Vacuum) as previously described[29, 31]. Briefly, the deposition chamber is a 240 mm diameter cylinder with a height of 33 mm. The top of the reactor is covered with a 25 mm thick quartz plate, allowing for observation of the sample throughout deposition. Liquid monomer (1,3,5 trivinyl-trimethyl-cyclotrisiloxane, 99% Gelest) and initiator (tertbutyl peroxide, 98% Aldrich) were utilized without further purification. The monomer was vaporized in a metal crucible maintained at 80 ± 2 °C and vapor flow

metered to the reactor through a mass flow controller (Model 1152, MKS). The initiator was placed in a sealed Pyrex^{tm} container at room temperature and vapors fed to the reactor through a second mass flow controller (Model 1179A, MKS). Gaseous monomer and initiator were premixed and fed through a port in the side of the reactor cylinder where they then passed through a distribution baffle plate to ensure uniform flow over the deposition area.

Within the reactor, a resistively heated filament array, 20 mm above the substrate, was utilized to break down the initiator into radical species. Filament temperature was measured by a thermocouple (Type K, AWG 36, Omega Engineering) directly attached to one of the filament wires. Pressure within the chamber was measured by a capacitance diaphragm gauge and controlled through use of a throttling butterfly valve (Intellisys, NorCal) connected to an auto-tuned digital controller (Intellisys, NorCal).

Samples were deposited on either 100 mm diameter IR transparent silicon wafers (WaferWorld) or 50 μm diameter gold wire in direct contact with a backside cooled substrate stage within the reactor. In order to remove contaminants, all silicon samples were ultrasonicated for 10 minutes in deionized water, rinsed with isopropyl alcohol, and dried with nitrogen. Substrate temperature was maintained with an accuracy of ± 2 °C throughout the deposition by circulation of heated silicon oil. Film growth was observed *in situ* through use of a 633 nm laser source (JDS Uniphase), with reflectance intensity measured by a Metrologic detector. Interferometric cycle thickness was calibrated using ellipsometer modeling as described below.

Table 3-1, below, shows reactor conditions for all iCVD film samples analyzed in this paper.

Label	Pressure (mTorr)	Stage Temperature (Kelvin)	Filament Temperature (Kelvin)	Monomer Flowrate (sccm)	Initiator Flowrate (sccm)
A	350	328	773	5	0.5
B	350	333	773	5	0.5
C	350	353	773	5	0.5
D	450	333	773	5	0.5
E	350	308	773	5	0.5

Table 3-1. Reactor conditions for deposition of iCVD polymer films

3.3.2 Material Testing

Dielectric measurements were made using a mercury probe (Materials Development Corp.) driven by a Keithley 236 source measurement unit. A capacitance vs. voltage curve was generated and the dielectric constant calculated from the accumulation capacitance of the sample. Sample thickness and refractive index were measured through the use of a variable angle spectroscopic ellipsometer (J.A. Woollam M-2000, xenon light source). A Cauchy-Urbach model was utilized to obtain a non-linear least squares fit of data obtained at three (65°, 70°, 75°) angles and 225 wavelengths. Electrical resistance measurements were made utilizing a Keithley 617 Electrometer attached to the sample by adhesive electrodes (Tyco Healthcare) of known contact area. Sample resistivity was then calculated by multiplying the measured resistance by the ratio of the electrode area to the sample thickness (as determined by spectroscopic ellipsometry). Solubility testing was performed by immersion of thin film samples, on silicon substrates, in the stated solvent of 30 minutes, followed by drying with room temperature nitrogen. Film thickness was measured by spectroscopic ellipsometry before and after immersion.

Coating adhesion to silicon wafer substrates was determined using ASTM tape test D3359-02. For this adhesion test, a grid of 1 mm squares was cut into the sample and adhesive tape (P99 polyester tape, Pemacel) was applied and rapidly removed. The sample was then visually inspected to determine if any loss of adhesion between any of the small squares of coating and the surface had occurred. Testing was performed before and after boiling coated silicon wafer samples in deionized water for 60 minutes.

Fourier transform infrared spectroscopy (FTIR) was performed on a Nicolet Nexus 870 ESP spectrometer in normal transmission mode. A DTGS KBr detector was utilized over the range of 400 to 4000 cm^{-1} with a 4 cm^{-1} resolution. Measurements were averaged over either 64 or 128 scans. All samples were baseline corrected and thickness normalized to allow for accurate comparison. Scanning electron micrographs were generated using a FEI/Phillips XL30 FEG ESEM in environmental scanning mode. ESEM samples were examined as deposited, without addition of an evaporated metal overcoat. Atomic force microscopy (AFM) was performed on a Digital Instruments 3100 AFM with a type 4 controller utilizing a sample area of 1.5μm by 1.5μm.

Electrically biased soak testing was performed by Innersea Technology Inc. (Bedford, MA). Briefly, samples were deposited on a single side of 1 cm^2 pieces of silicon wafer to a thickness of 5 μm. In order to remove contaminants, samples were ultrasonicated for 10 minutes in deionized water, rinsed with isopropyl alcohol, and dried with nitrogen prior to coating deposition. Each square was then attached to a backside electrode and the sides and back of the sample insulated using silicone rubber to ensure that current could only pass to the backside electrode through the deposited coating. Samples were then placed on leads and suspended in test tubes filled with saline solution

as shown in Figure 3-2. Each tube was also fitted with an electrode suspended in the saline solution, and a sweeping electrical bias of +5V to -5V was maintained between this free electrode and those present on each of the samples under test. The leakage current through each of the samples was then measured every 24-72 hours at both +5V and -5V and sample electrical resistance was subsequently calculated and recorded.

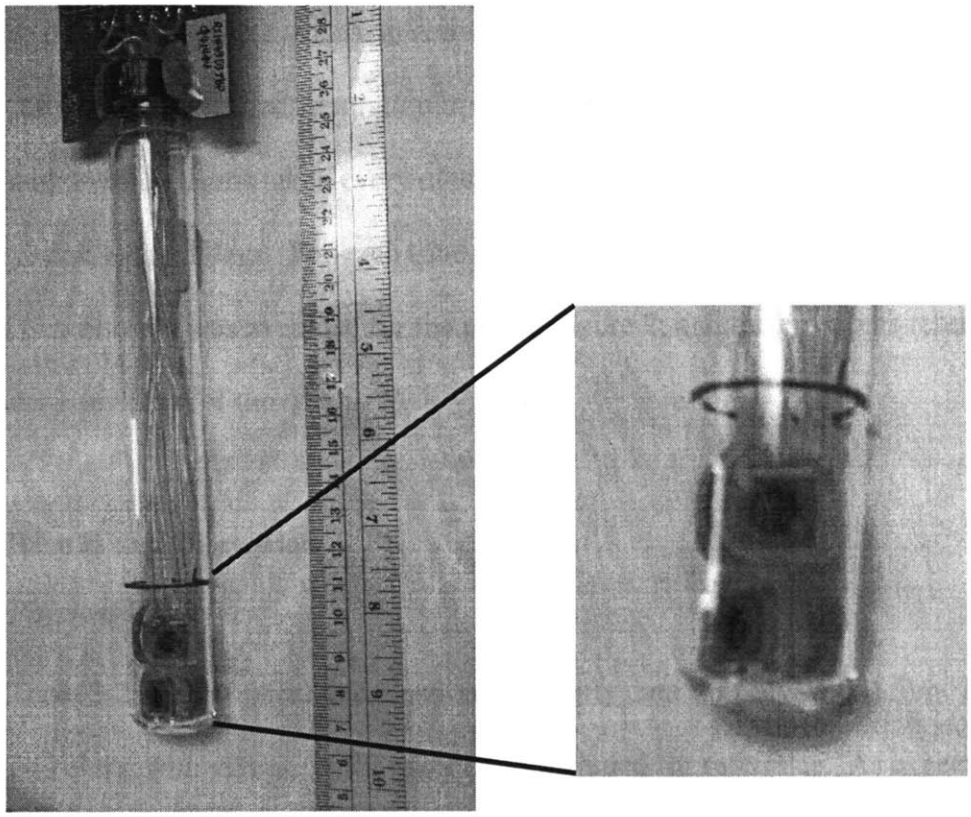

Figure 3-2: Electrically biased saline soak test setup for durability testing of poly(V_3D_3) coatings. Enlargement shows detail of how samples were assembled and electrically isolated.

3.3.3 Neuron Compatibility Testing

Coated glass slides were placed in suspensions of PC12 cells over a period of 12 days. The PC12 cell line was obtained from American Type Culture Collection (ATCC) and cultured in F-12K medium (ATCC) supplemented with 15% horse serum (ATCC),

2.5% fetal bovine serum (BioWhittaker), and 25 units/mL penicillin-streptomycin (Hyclone) at 37 °C and 5% CO_2. For neurocompatibility experiments, five coated glass slides were placed in small polystyrene petri dishes (Fisher; one slide in each dish) along with 12 mL of cell suspension in each dish. Five uncoated glass slides in similar petri dishes served as controls. Cell culture conditions utilized for this study provided for the growth of PC12 neurons in suspension above the substrates, though contact due to cell settling did occur. The cell concentration in each dish was monitored over a 12 day period, with measurements taken every other day. Medium changes were carried out in each petri dish every 3 days. For each time point, the cell concentration from the five samples (or controls) was averaged for the plot in Figure 7, and the error bars represent the standard deviation of the data.

3.4 Results and Discussion

3.4.1 Physical Properties

Table 3-2 shows optical and electronic property data for poly(V_3D_3) film "B" (Table 3-1) along with values for PE and PDMS included for reference. As expected, all properties of the new material fall between those of PE and PDMS, confirming the assertion that the material will behave as a PE – siloxane copolymer. Of these properties, the most important to the application is the electrical resistivity. In order to both ensure recording from single neurons and to increasing recording sensitivity, the electrical resistance of the passivation coating should be as high as possible. Parylene-C, the current electrical insulation material of choice for these implants [16, 34-36], has a bulk resistivity on the order of 10^{15} Ω–cm, slightly lower than that of the poly(V_3D_3). This

differential should allow for deposition of thinner passivation coatings that will provide the same level of electrical insulation to the device.

Material	Dielectric Constant	Refractive Index	Resistivity (Ω-cm)
Poly(V_3D_3)	2.5 ± 0.2	1.465 ± 0.01	4 (± 2) X 10^{15}
Polyethylene	2.3 ± 0.02	1.49 – 1.54	1 X 10^{14}
Polydimethylsiloxane	2.6 ± 0.2	1.40	1 X 10^{16}
Parylene - C	3.0 ± 0.15	1.64	1 X 10^{15}

Table 2: Optical and electrical properties of poly(V_3D_3) along with those of polyethylene, polydimethylsiloxane, and Parylene-C for comparison.

The material properties of poly(V_3D_3) were found to be insensitive to changes in deposition conditions over the range of conditions reported in Table 3-1, samples A-D. The only exception appears to be when substrate temperatures are reduced below a rector pressure dependant threshold value. For a deposition pressure of 350 mtorr, this threshold was observed to be ~323 K. Below this level a decrease in bulk resistivity of up to two orders of magnitude is observed. A resistivity of ~1 X 1013 Ohm-cm was obtained for samples deposited at a stage temperature of 308K (condition E, Table 1). The loss of electrical resistance is hypothesized to originate with the entrainment of some small molecules in the polymerized film when surface temperature is low. Upon reactor blowdown following the deposition process, vaporization of the entrained molecules leads to defects which can observed by optical microscopy as micron-size disk-shaped

voids in the coating. The entrained small molecules could be either short oligomers of the polymer, or possibly a single monomer unit which has been initiated and terminated without further monomer addition. Condensation of the pure monomer is less likely, as the partial pressure of monomer in the reactor, 280 mTorr, is significantly below its vapor pressure of ~500 mTorr at the substrate temperature.

Table 3-3 presents data on the adhesion of poly(V_3D_3) films, "B" (Table 3-1), to silicon wafer substrates. Note that the native oxide was not removed prior to the iCVD coating step. Substrate adhesion is very important for the long term stability of implanted probes as coating delamination can quickly lead to corrosion and device failure[37]. Coating adhesion was evaluated for films both less than and greater than 100 nm in thickness, since the organizational structure of polymer films deposited on crystalline substrates has been reported to be greatly affected by the crystalline lattice structure in the first 50-200nm[38, 39]. In all cases, a rating of 5B, no loss of coating adhesion observable, was obtained from ASTM tape test D3359-02. In order to make an initial assessment of whether long term immersion in an aqueous environment would impact adhesion, samples were then boiled for 30 minutes in deionized water. Once again no loss of film adhesion was observed upon testing.

Sample Thickness	Rating (as deposited)	Rating (after boiling)
61 ± 2nm	5B (0% removal)	5B (0% removal)
315 ± 6nm	5B (0% removal)	5B (0% removal)

Table 3-3. ASTM tape test D3359-02 adhesion data for poly(V_3D_3) deposited on silicon wafer substrates. 5B rating indicates best possible adhesion to substrate as measurable by this assay.Measurements were taken before and after boiling in deionized water for 60 minutes.

Figure 3-3 displays a scanning electron microscopy (SEM) image of a nominally 50 μm diameter gold wire coated with 2-3 μm of poly(V_3D_3) deposited at condition "B" from Table 1. The wire has been bent into a loop of ~250 μm in diameter to demonstrate the flexibility of the thin film coating. As can be seen from the figure, no cracking or buckling in the film is observable. Flexibility is an important property for the coating of neural probe assemblies which typically have multiple lead wires attaching them to either locally implanted or external electronics. The ability to coat these leads along with the device would be a significant advantage over Parylene-C which is too brittle for such an application[36]. The flexibility of the poly(V_3D_3) is not surprising when the polymer film is considered as a siloxane copolymer. Siloxane materials are noted for their flexibility and elastomeric properties.

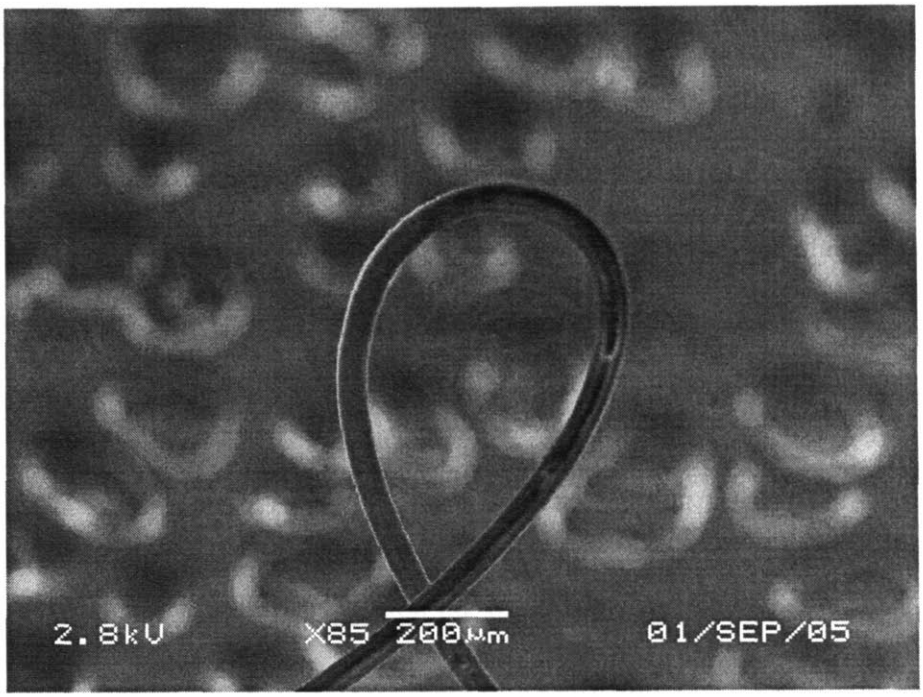

Figure 3-3. Scanning electron micrograph of 50 µm diameter gold wire coated with 2-3 µm of poly(V_3D_3). Wire is bent into a ~250 µm diameter loop without evidence of film cracking or buckling.

Figure 3-4 presents an atomic force micrograph (AFM) of poly(V_3D_3) film "C" (Table 3-1) deposited on a silicon wafer substrate to a thickness of ~250 nm. The overall root mean square (RMS) roughness of the sample is only 0.4 nm, comparing well to the 0.15 nm observed for polished silicon wafers. In addition, the peak to peak roughness (not shown) is no greater than 0.9 nm. This indicates that the low RMS figure is due to a film of uniformly low surface roughness, not a smooth film with occasional large peaks/flaws. This is important to ensure that no point imperfections are present in the film. Additionally, while the AFM data was obtained from analysis of a sample deposited at condition C, there was very little variation in surface roughness observed in samples deposited at conditions listed in Table 3-1. All tested samples were within ±0.25 nm RMS roughness of the above data. The low roughness of thin films of the polymer is

indicative of an amorphous material, though confirmation of this through X-ray powder diffraction (XRD) or differential scanning calorimetry (DSC) is not possible due to the small sample sizes. An amorphous film is also consistent with the interpretation of the chemical structure as a PE-siloxane copolymer. While PE is a semi-crystalline polymer, it is theorized that the presence of the siloxane side groups within the poly(V3D3) would most likely prevent the PE chains from forming crystalline domains. These observations are also consistent with the film flexibility observed in Figure 2; a semi-crystalline material would be likely to display some degree of brittle cracking under strain. An amorphous polymer structure is beneficial for electrically insulating films as material properties will be isotropic and the possibility of locally high electrical conduction at crystalline grain boundaries is avoided.

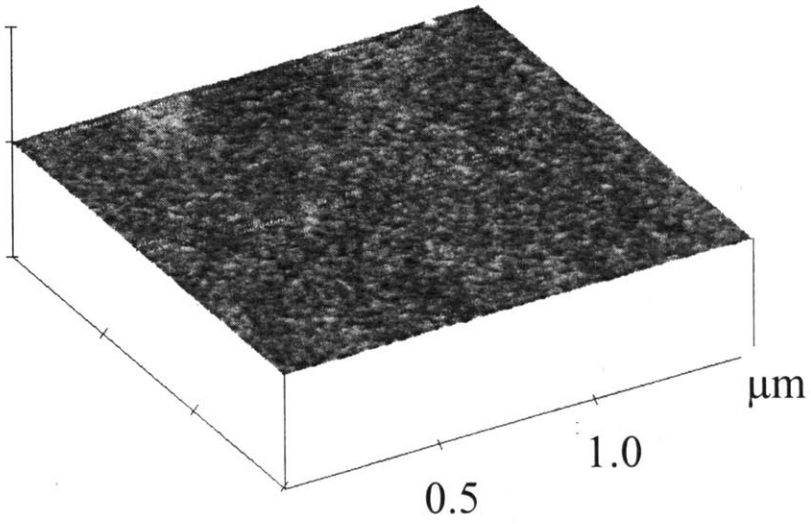

Figure 3-4. Atomic Force Micrograph of poly(V_3D_3) film "C" deposited on a silicon wafer. Sample has an overall RMS roughness of 0.4 nm with a peak to peak roughness of <0.9nm.

3.4.2 Material Stability

Figure 3-5 displays two FTIR spectra of a poly(V_3D_3) film deposited at condition B. The bottom spectra is that of the as-deposited film, while the top spectra is of the same film after boiling at atmospheric pressure in deionized water for one hour. A detailed analysis of the IR absorptions present has been previously reported[33]. No change in FTIR spectra of the material is observed, indicating that there are no hydrolytically labile moieties present in the film which could be degraded overtime in an aqueous environment. Were the film to react with water, new absorptions associated with hydroxyl groups would be observed between both 3400-3600 cm^{-1} and 1000-1100 cm^{-1} [40]. The hydrolytic stability of this material is not unexpected when again considering the poly(V_3D_3) within the context of a PE – siloxane copolymer. Both components are unaffected chemically by aqueous environments.

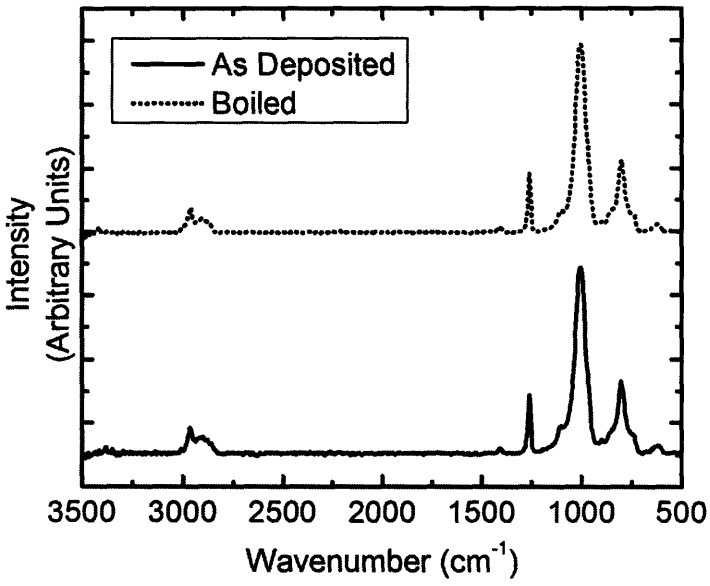

Figure 3-5. FTIR spectra of a poly(V_3D_3) film "B" before and after boiling for 60 minutes in deionized water. No change in spectra is apparent.

Table 3-4 presents solubility data on poly(V_3D_3) films prepared at condition A in a variety of common solvents. Resistance to polar solvents is obviously of most importance for permanently implantable materials. However, cholesterols and other fatty acids in the blood can act as non-polar solvents, slowly leaching away oil soluble materials. As shown by the data, poly(V_3D_3) films show no solubility in either polar or non-polar solvents, indicating that coating loss due to solvation within the body will not likely be a factor. These results confirm that the crosslinked structure of the poly(V3D3) films is effective in retaining all deposited material and that low molecular weight chains, which would be solubilized, are not present.

Solvent	**Initial Thickness**	**Final Thickness**
Deionized Water	391 ± 8 nm	397 ± 8 nm
Isopropyl Alcohol	410 ± 12 nm	408 ± 12nm
Acetone	418 ± 10nm	424 ± 10nm
Dimethyl Sulfoxide	438 ± 8 nm	431 ± 8 nm
Tetrahydrofuran	292 ± 6 nm	293 ± 6 nm

Table 3-4. Film thickness of samples before and after 30 minute soak in specified solvent. Thickness measured by spectroscopic ellipsometry with accuracy given.

Stability of coating electrical properties under physiological conditions is of paramount importance for the application. Figure 3-6 presents a plot of electrical resistance vs. time for five thin film poly(V_3D_3) samples from June 2004 through February 2006. These samples were deposited at condition "B" (Table 3-1). As described

in Section 3.3.2, these samples were immersed in physiological saline and had a constant sweeping electrical bias of +5V to -5V applied across them. Note that due to film area vs. film thickness considerations a resistivity of 10^{15} Ω–cm corresponds to a measured resistance of 1.1 X 10^{12} Ω, indicating that all five samples fall in the range of electrical resistivity previously presented in Table 3-2. These data indicates that, even after more than two and a half years of simulated implantation, the electrical properties of the five samples have not degraded. Indeed, the small variations in resistance observed seem to track between the samples, indicating that the changes are more likely due to small fluctuations in calibration of the electrometer utilized to take the measurements. It should be noted that three additional samples were placed under test along with these five, all three of which failed electrically within the first two weeks. Examination of these failed samples indicated that they were point failures due to the presence of particulate contaminants on the substrate surface prior to coating, not failures due to degradation of the coating itself. This particulate contamination likely occurred after sample cleaning procedures as depositions were no performed in a clean room environment. Such an environment will be utilized during future neural implant device manufacture to avoid this failure mode.

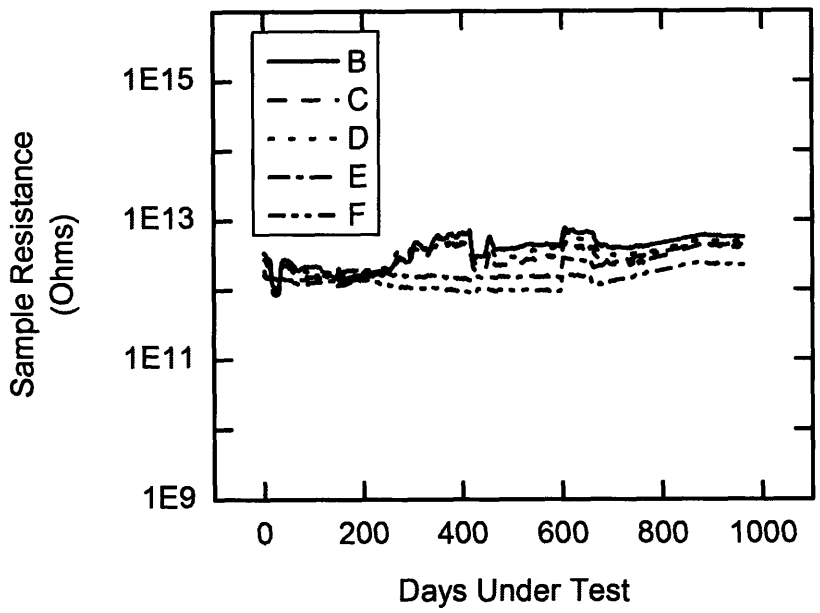

Figure 3-6. Electrical resistance of poly(V_3D_3) samples under simulated bio-implanted conditions and constant electrical bias. Samples show no degradation in electrical resistance over a period of greater than two and a half years.

3.4.3 Neuron Compatibility

The compatibility of poly(V_3D_3) thin films to neurons was assessed by culturing PC12 neurons in the presence of glass slides coated with the material. PC12 cultures in the presence of uncoated glass slides served as a negative control. Figure 3-7 shows the progression of cell concentration as a function of time over a 12-day period. There is no statistically significant (as evaluated by 95% confidence t test[41]) difference between sample and control cell concentration data, indicating that contact with poly(V_3D_3) does not affect the growth characteristics of PC12 neurons. In both sample and control, the PC12 cells retained a rounded morphology and did not adhere to the dish or glass surfaces. This behavior is consistent with the expected behavior of PC12 cells in the presence of serum but in the absence of cell adhesion proteins or neurotrophic factors[42].

While this growth curve experiment is a first order assay for biocompatibility, the results nevertheless indicate that poly(V_3D_3) films do not retard cell growth due to factors such as cytotoxic chemical groups, entrained monomers, or unreacted initiator. Additionally, previous work with related film chemistries has demonstrated the tethering of bioactive molecules, such as the peptide sequence RGD, to the surface of iCVD films through vinyl moieties not consumed during polymerization[43]. This or related approaches can be utilized to further increase the biocompatibility of p(V_3D_3).

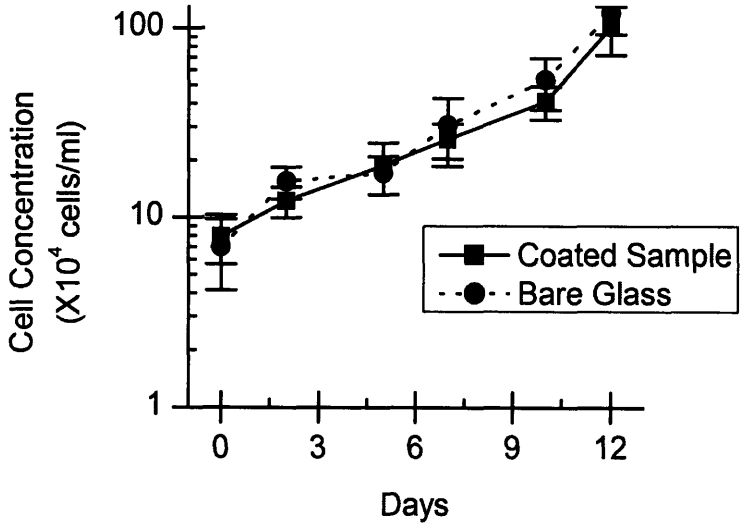

Figure 3-7. PC12 neuron growth in the presence of uncoated and V_3D_3 coated glass substrates. No significant difference in cell growth is observed, indicating that poly(V_3D_3) is non-cytotoxic to PC12 neurons.

3.5 Conclusions

In this chapter, thin films of poly(V_3D_3) deposited by iCVD have been demonstrated to possess the material properties and long term stability for electrically insulating neural recording arrays. The material has also been shown to have excellent adhesion to silicone substrates and a high degree of flexibility, both necessary properties for an ideal neural probe insulating material. It has been demonstrated that this polymer

in many ways behaves as a copolymer of polyethylene and a polysiloxane, as would be predicted from its chemical structure. Poly(V_3D_3) has a bulk electrical resistivity in excess of 10^{15} Ω–cm, allowing for films as thin as 5μm to provide the required degree of electrical insulation for the application. This value falls between those observed in PE and PDMS, as do the refractive index and dielectric constant of the material. iCVD deposited poly(V_3D_3) shows no spectroscopic change due to hydrolysis when exposed to a 100 °C aqueous environment. Negligible solubility in a wide range of solvents has been demonstrated, assuring that the coating will not be dissolved by either hydrophilic or hydrophobic materials it may encounter when implanted in the cortex. In addition, it has been shown that the electrical properties of the material are maintained, with no degradation, for over two and a half years under simulated implant conditions. Lastly, biocompatibility studies with PC12 neurons demonstrate that this material is non-cytotoxic and does not influence cell proliferation. These data provide initial indications of biocompatibility.

Future work with this material will focus on both short and long term *in vivo* testing to better understand how the coating will behave in an active biological environment. In addition, the surface of the material will be modified for attachment of bioactive molecules, such as the peptide RGD, to increase cell affinity for the material surface. This modification will maximize the integration and stability of the coating within the cellular matrix after implantation.

3.6 Acknowledgment

The authors acknowledge the support of the NIH under contract No. NO1-NS2-2347. This work also made use of the MRSEC shared facilities supported by NSF grant

No. DMR-9400334. The authors thank Anilkumar Achyuta for performing the cell compatibility experiments.

3.7 References

1. Santhanam, G.; Ryu, S. I.; Yu, B. M.; Afshar, A.; Shenoy, K. V., A high-performance brain-computer interface. *Nature* **2006,** 442, (7099), 195-198.
2. Taylor, D. M.; Tillery, S. I. H.; Schwartz, A. B., Direct cortical control of 3D neuroprosthetic devices. *Science* **2002,** 296, (5574), 1829-1832.
3. Beard, R. B.; Hung, B. N.; Schmukler, R., Biocompatibility Considerations at Stimulating Electrode Interfaces. *Annals of Biomedical Engineering* **1992,** 20, (3), 395-410.
4. Szarowski, D. H.; Andersen, M. D.; Retterer, S.; Spence, A. J.; Isaacson, M.; Craighead, H. G.; Turner, J. N.; Shain, W., Brain responses to micro-machined silicon devices. *Brain Research* **2003,** 983, (1-2), 23-35.
5. Edell, D. J.; Toi, V. V.; McNeil, V. M.; Clark, L. D., Factors Influencing the Biocompatibility of Insertable Silicon Microshafts in Cerebral-Cortex. *Ieee Transactions on Biomedical Engineering* **1992,** 39, (6), 635-643.
6. Vetter, R. J.; Williams, J. C.; Hetke, J. F.; Nunamaker, E. A.; Kipke, D. R., Chronic neural recording using silicon-substrate microelectrode arrays implanted in cerebral cortex. *Ieee Transactions On Biomedical Engineering* **2004,** 51, (6), 896-904.
7. Schmidt, S.; Horch, K.; Normann, R., Biocompatibility of Silicon-Based Electrode Arrays Implanted in Feline Cortical Tissue. *Journal of Biomedical Materials Research* **1993,** 27, (11), 1393-1399.
8. Rousche, P. J.; Normann, R. A., Chronic recording capability of the Utah Intracortical Electrode Array in cat sensory cortex. *Journal of Neuroscience Methods* **1998,** 82, (1), 1-15.
9. Polikov, V. S.; Tresco, P. A.; Reichert, W. M., Response of brain tissue to chronically implanted neural electrodes. *Journal Of Neuroscience Methods* **2005,** 148, (1), 1-18.
10. Rennaker, R. L.; Street, S.; Ruyle, A. M.; Sloan, A. M., A comparison of chronic multi-channel cortical implantation techniques: manual versus mechanical insertion. *Journal Of Neuroscience Methods* **2005,** 142, (2), 169-176.
11. Griffith, R. W.; Humphrey, D. R., Long-term gliosis around chronically implanted platinum electrodes in the Rhesus macaque motor cortex. *Neuroscience Letters* **2006,** 406, (1-2), 81-86.
12. Rutten, W. L. C., Selective electrical interfaces with the nervous system. *Annual Review Of Biomedical Engineering* **2002,** 4, 407-452.
13. Nordhausen, C. T.; Maynard, E. M.; Normann, R. A., Single unit recording capabilities of a 100 microelectrode array. *Brain Research* **1996,** 726, (1-2), 129-140.
14. Eversmann, B.; Jenkner, M.; Hofmann, F.; Paulus, C.; Brederlow, R.; Holzapfl, B.; Fromherz, P.; Merz, M.; Brenner, M.; Schreiter, M.; Gabl, R.; Plehnert, K.;

Steinhauser, M.; Eckstein, G.; Schmitt-Landsiedel, D.; Thewes, R., A 128x128 CMOS biosensor array for extracellular recording of neural activity. *Ieee Journal Of Solid-State Circuits* **2003,** 38, (12), 2306-2317.

15. Navarro, X.; Krueger, T. B.; Lago, N.; Micera, S.; Stieglitz, T.; Dario, P., A critical review of interfaces with the peripheral nervous system for the control of neuroprostheses and hybrid bionic systems. *Journal Of The Peripheral Nervous System* **2005,** 10, (3), 229-258.
16. Xu, C. Y.; Lemon, W.; Liu, C., Design and fabrication of a high-density metal microelectrode array for neural recording. *Sensors And Actuators A-Physical* **2002,** 96, (1), 78-85.
17. Bhat, S. V., *Biomaterials*. First ed.; Narosa Publishing House: New Delhi, India, 2002.
18. Chawla, A. S., Evaluation of Plasma Polymerized Hexamethylcyclotrisiloxane Biomaterials Towards Adhesion of Canine Platelets and Leukocytes. *Biomaterials* **1981,** 2, (2), 83-88.
19. Lewis, H. G. P.; Edell, D. J.; Gleason, K. K., Pulsed-PECVD films from hexamethylcyclotrisiloxane for use as insulating biomaterials. *Chemistry of Materials* **2000,** 12, (11), 3488-3494.
20. Lewis, H. G. P.; Casserly, T. B.; Gleason, K. K., Hot-filament chemical vapor deposition of organosilicon thin films from hexamethylcyclotrisiloxane and octamethylcyclotetrasiloxane. *Journal of the Electrochemical Society* **2001,** 148, (12), F212-F220.
21. Chu, P. K.; Chen, J. Y.; Wang, L. P.; Huang, N., Plasma-surface modification of biomaterials. *Materials Science & Engineering R-Reports* **2002,** 36, (5-6), 143-206.
22. Favia, P.; d'Agostino, R., Plasma treatments and plasma deposition of polymers for biomedical applications. *Surface & Coatings Technology* **1998,** 98, (1-3), 1102-1106.
23. Lahann, J., Vapor-based polymer coatings for potential biomedical applications. *Polymer International* **2006,** 55, (12), 1361-1370.
24. Yoshida, M.; Langer, R.; Lendlein, A.; Lahann, J., From advanced biomedical coatings to multi-functionalized biomaterials. *Polymer Reviews* **2006,** 46, (4), 347-375.
25. Yasuda, H., *Plasma Polymerization*. Academic Press: 1985.
26. Limb, S. J.; Gleason, K. K.; Edell, D. J.; Gleason, E. F., Flexible fluorocarbon wire coatings by pulsed plasma enhanced chemical vapor deposition. *Journal of Vacuum Science & Technology a-Vacuum Surfaces and Films* **1997,** 15, (4), 1814-1818.
27. Pierson, H. O., *Handbook of Chemical Vapor Deposition*. 2nd ed.; William Andrew Publishing: Norwich, N.Y., 1999.
28. Lau, K. K. S.; Gleason, K. K., Particle surface design using an all-dry encapsulation method. *Advanced Materials* **2006,** 18, (15), 1972-+.
29. Chan, K.; Gleason, K. K., Initiated CVD of poly(methyl methacrylate) thin films. *Chemical Vapor Deposition* **2005,** 11, (10), 437-443.

30. Mao, Y.; Gleason, K. K., Hot filament chemical vapor deposition of poly(glycidyl methacrylate) thin films using tert-butyl peroxide as an initiator. *Langmuir* **2004,** 20, (6), 2484-2488.
31. Chan, K.; Gleason, K. K., Initiated chemical vapor deposition of linear and cross-linked poly(2-hydroxyethyl methacrylate) for use as thin-film hydrogels. *Langmuir* **2005,** 21, (19), 8930-8939.
32. Lau, K. K. S.; Gleason, K. K., Initiated chemical vapor deposition (iCVD) of poly(alkyl acrylates): An experimental study. *Macromolecules* **2006,** 39, (10), 3688-3694.
33. O'Shaughnessy, W. S.; Gao, M. L.; Gleason, K. K., Initiated chemical vapor deposition of trivinyltrimethylcyclotrisiloxane for biomaterial coatings. *Langmuir* **2006,** 22, (16), 7021-7026.
34. Bradley, D. C.; Troyk, P. R.; Berg, J. A.; Bak, M.; Cogan, S.; Erickson, R.; Kufta, C.; Mascaro, M.; McCreery, D.; Schmidt, E. M.; Towle, V. L.; Xu, H., Visuotopic mapping through a multichannel stimulating implant in primate V1. *Journal Of Neurophysiology* **2005,** 93, (3), 1659-1670.
35. Yamagishi, F. G., Investigation Of Plasma-Polymerized Films As Primers For Parylene-C Coatings On Neural Prosthesis Materials. *Thin Solid Films* **1991,** 202, (1), 39-50.
36. Schmidt, E. M.; McIntosh, J. S.; Bak, M. J., Long-Term Implants Of Parylene-C Coated Microelectrodes. *Medical & Biological Engineering & Computing* **1988,** 26, (1), 96-101.
37. Troyk, P. R.; Watson, M. J.; Poyezdala, J. J., Humidity Testing Of Silicone Polymers For Corrosion Control Of Implanted Medical Electronic Prostheses. *Acs Symposium Series* **1986,** 322, 299-313.
38. Wang, D.; Ishida, H., Probing friction and adhesion properties of poly(vinyl methylether) homopolymer and blend films under nano-confinement using atomic-force microscopy. *Comptes Rendus Chimie* **2006,** 9, (1), 90-98.
39. Itagaki, H.; Nishimura, Y.; Sagisaka, E.; Grohens, Y., Entanglement of polymer chains in ultrathin films. *Langmuir* **2006,** 22, (2), 742-748.
40. D. Lin-Vien, N. C., W. Fately, J. Grasselli, *The Handbook of Infrared and Ramman Characteristic Frequencies of Organic Molecules*. Academic Press: San Diego, 1991.
41. Montgomery, D. C., *Design and Analysis of Experiments*. John C. Wiley & Sons: New York, 1997.
42. Pollock, J. D.; Krempin, M.; Rudy, B., Differential-Effects Of Ngf, Fgf, Egf, Camp, And Dexamethasone On Neurite Outgrowth And Sodium-Channel Expression In Pc12 Cells. *Journal Of Neuroscience* **1990,** 10, (8), 2626-2637.
43. Murthy, S. K.; Olsen, B. D.; Gleason, K. K., Peptide attachment to vapor deposited polymeric thin films. *Langmuir* **2004,** 20, (11), 4774-4776.

Chapter Four

Initiated Chemical Vapor Deposition (iCVD) of a surface modifiable copolymer for covalent attachment and patterning of nucleophilic ligands*

* Submitted to Macromolecular Rapid Communications

4.1 Abstract

Many novel areas of biological investigation require the patterned immobilization of bioactive ligands. In this chapter, patterned functionalization is demonstrated using pentafluorophenyl methacrylate (PFM)/ ethylene glycol diacrylate (EGDA) copolymeric thin films synthesized by initiated chemical vapor deposited (iCVD). The PFM presents a side chain moiety, pentafluorophenyl ester, an excellent leaving group which allows the attachment of nucleophilic ligands in a single chemical step. The EGDA functions as a crosslinking agent, stabilizing the functional thin film coatings against dissolution in biologically relevant solvents following modification. Functionalization of iCVD PFM-EGDA copolymer with aminoethoxy ethanol converts the PFM side chain from hydrophobic to hydrophilic and the observed contact angle with water is reduced by nearly 20^{o}. Patterned surface functionalization through microcontact printing of fluorescently labeled amines is also demonstrated. These ligands remain immobilized even after repeated solvent rinses. In addition, the synthesis of this material by iCVD opens the door to integrate this facile modification approach within a large range of thin film materials, including hydrogels and other functional acrylates.

4.2 Introduction

Surface modification of polymers with signaling molecules and attachment ligands is important for improving both the functionality and biocompatibility of biomaterials[1, 2]. Specific applications include attachment of targeted cells[3], stem cell differentiation [4, 5], and improved bio-acceptance of implanted materials[6, 7]. When ligands can be patterned onto biomaterial surfaces, additional applications such as bio-sensor

arrays[8] and cell immobilization and sorting[8, 9] are also possible. A common approach for creating easily modified biomaterial polymers is the inclusion of reactive side groups which can be utilized for single step protein immobilization[10]. One such moiety is pentafluorophenyl ester, which is highly reactive toward nucleophiles[11-13]. Covalent attachment of proteins and peptides through amino acid residues containing nucleophilic side chains, such as lysine, can be easily achieved (Fig. 4-1). The low charge density of the pentafluorophenyl anion makes it an excellent leaving group in this reaction. Moreover, it has been recently demonstrated that the pentafluorophenyl ester moiety reacts significantly faster with amines versus other nucleophilic groups, such as alcohols or even water. This opens the possibility to use this molecule for peptide attachment reactions in aqueous media[14].

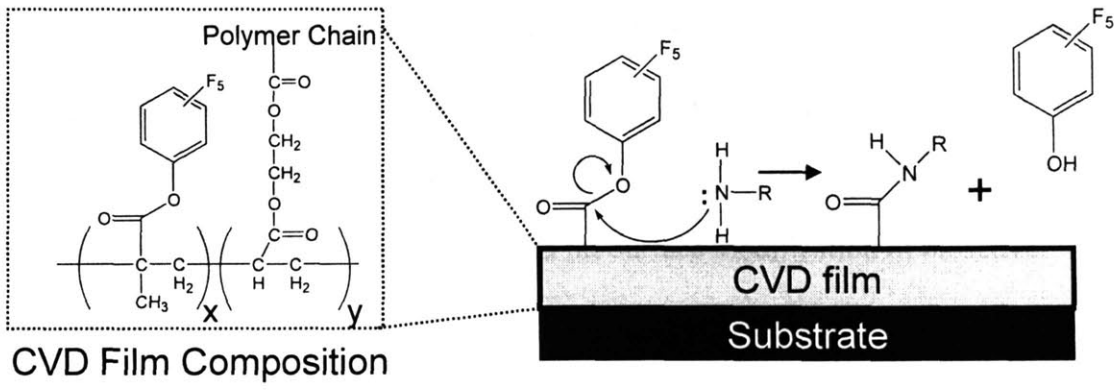

Figure 4-1. Copolymer structure and surface modification scheme demonstrating the single step attachment of any amine containing ligand.

Previous work has demonstrated pyrolytic chemical vapor deposition (CVD) of a pentafluorophenyl ester containing parylene derivative[12, 13], as well as plasma enhanced CVD of PFM[11]. In this work, thin films of pentaflurophenyl methacrylate (PFM) and its copolymer with ethylene glycol diacrylate (EGDA) (Fig. 4-1) are synthesized by initiated CVD (iCVD). In part, the choice of iCVD is motivated by the desire to avoid conditions

which have the potential to damage sensitive substrates or the growing films, such as high surface temperatures or bombardment of the surface by reactive ions[15]. The iCVD process permits the deposition of conformal thin films of polymer on room temperature substrates[16, 17]. In addition, as a low energy free radical process, iCVD allows for copolymerization of vinyl containing monomers with full retention of delicate side groups which may be damaged by alternate CVD processes[16, 17]. The retention of the pendent functionality of PFM enables both bulk and patterned functionalization of iCVD PFM/EGMA copolymers as demonstrated in this chapter.

An additional motivation for adopting iCVD is the ease of forming copolymers. In this section, copolymerization of PFM with the crosslinker EDGA creates a robust insoluble film allowing for both bulk and surface functionalization of the material. Copolymerization with additional iCVD monomers is envisioned for creating surfaces having more complex biological functionality. One future possibility includes a functionalized hydrogel, such as hydroxyethyl methacrylate (HEMA)[16] copolymerized with PFM, which could be of great utility in the surface modification of bioactive membranes.

4.3 Experimental Part

4.3.1 Sample Preparation

Material samples were prepared in a custom built vacuum reactor as previously described in detail[16-18]. PFM (95%, Monomer Polymer) and EGDA (97%, Polysciences) monomers and tert-butyl peroxide (95%, Aldrich) initiator were utilized without further purification. The initiator flowrate was maintained at 0.25 sccm through an MKS 1479

flow controller, while both monomers were allowed to free flow into the reactor from temperature controlled crucibles. Monomer flowrates were varied through selection of crucible temperature. PFM flowrate was maintained at 2 sccm (crucible at 45 °C) for all depositions, excluding that of EGDA homopolymer, while EGDA flowrate varied from 0.2 – 0.8 sccm (crucible 50-70 °C). Reactor pressure was maintained at 250 mtorr for all depositions. All samples were deposited on IR transparent silicon wafers (Waferworld) maintained at 35 °C through backside coolant circulation. The initiator was broken down to free radical species over a resistively heated Nichrome filament (Omega) maintained at a temperature of 250 °C. Film growth was observed *in situ* through interferometry and used to obtain final thickness between 200-250 nm for all samples.

4.3.2 Sample Modification

Bulk functionalization of copolymer samples was performed with a 0.5 M solution of 2,2-aminoethoxy ethanol (98%, Aldrich) in ethanol (99.5%, Aldrich). Samples were immersed in solution and maintained at 50 °C for 12 hours. Patterned functionalization was performed using a 10 mM solution of fluorescein-5-thiosemicarbazide (Molecular Probes) in ethanol. This solution was applied to a PDMS microcontact stamp (prepared for a previous study[19]) using a cotton swab. The stamp was then dried with room temperature nitrogen and contacted to the surface of the copolymer film for 2 minutes. Following stamping, samples were rinsed 3 times with 15-30 ml room temperature ethanol (from a squirt bottle) to remove any unreacted ligand.

4.3.3 Sample Analysis

Sample thicknesses (200 - 250 nm) were measured through the use of a variable angle spectroscopic ellipsometer (J.A. Woollam M-2000, xenon light source). A

Cauchy-Urbach model was utilized to obtain a non-linear least squares fit of data obtained at either one (70°) or three (65°, 70°, 75°) angles and 225 wavelengths. Fourier transform infrared spectroscopy (FTIR) was performed on a Nicolet Nexus 870 ESP spectrometer in normal transmission mode. A DTGS KBr detector was utilized over the range of 400 to 4000 cm^{-1} with a 4 cm^{-1} resolution. Measurements were averaged over either 64 or 128 scans. All samples were baseline corrected and thickness normalized to allow for accurate comparison. Contact-angle measurements were performed on a goiometer equipped with an automatic dispenser (Model 500, Rame'-Hart). Optical micrographs were obtained on a Zeuss Axiovert 200 inverted microscope using FITC fluorescence illumination.

4.4 Results and Discussion

4.4.1 Polymer Film Characterization

Figure 4-2 displays the thickness normalized FTIR spectra of four iCVD polymers deposited from various ratios of pentafluorophenyl methacrylate (PFM) to ethylene glycol diacrylate (EGDA). The top spectrum is of the polymer resulting from deposition of PFM monomer alone. It contains four characteristic IR absorptions which indicate that the pentafluorophenyl ester moiety in the monomer has been preserved in the polymer. This most intense of these is the peak at 1523 cm^{-1}, an absorption characteristic of the C-C bonds within the benzene ring[20]. This peak appears at the top end of its normal range of 1400-1525 cm^{-1}, consistent with fluorine substitution of the phenyl moiety which can increase the absorption frequency of unsaturated C-C bonds by up to 35 cm^{-1} [20]. Absorptions associated with the carbonyl moiety (1785 cm^{-1}), the C-O

bond of the ester linkage (1069 cm^{-1}), and the C-F bonds (1000 cm^{-1}) are also apparent. Absorption associated with the vinyl C-C (1597 cm-1, 1408 cm-1) and C-H bonds (3000-3090cm^{-1})[18, 20] are not present in the p(PFM) spectrum, indicating that the vinyl moiety in the PFM monomer has reacted to form the polymer backbone. This consumption of the vinyl moiety through iCVD polymerization has been observed for multiple other polymers, including p(hydroxyethyl methacrylate) and p(trivinyltimethylcyclotrisiloxane), and has been demonstrated as indicative of free radical polymerization[16, 18]. The final item of note within the PFM homopolymer spectrum is the lack of significant additional IR absorptions, indicating a very homogenous polymer structure. This uniformity is unlike p(PFM) films created through plasma polymerization which display a great deal of variability in their resulting polymer structure as evidenced by the high number of IR absorptions present in their FTIR spectra[11].

(a

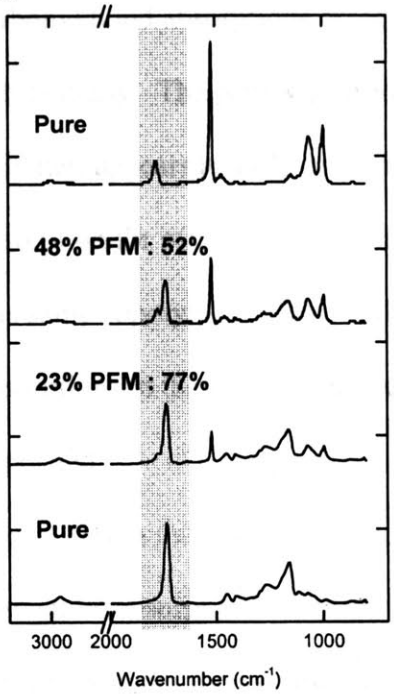

(b

Polymer Composition (% PFM)	PFM Carbonyl Peak	EDGA Carbonyl Peak
100%	1782	NA
48%	1776	1741
23%	1774	1737
0%	NA	1735

Figure 4-2. (a) IR spectra of four polymer compositions synthesized by iCVD. P(PFM-co-EGDA) films display characteristic absorptions of both homopolymers, though with slight shifts in peak location indicative of copolymerization. (b) Displays a table of the FTIR absorption frequencies (in cm^{-1}) of both PFM and EGDA carbonyl bonds as a function of film composition. A shift in these peak positions between the homo and copolymer spectra is observed verifying copolymerization.

The bottom spectrum in Figure 4-2 is that of the homopolymer p(EGDA) without the inclusion of any PFM. This spectrum contains two peaks, at 1735 cm^{-1} and 1165 cm^{-1}, which demonstrate the retention of the di-ester functionality within the p(EGDA) film[20]. Once again, the C-C and C-H absorptions associated with the vinyl moiety, present in the monomer, are not observed in the p(EGDA) spectrum. This indicates a polymer structure formed through free radical polymerization as with the p(PFM).

The two middle spectra in Figure 2 are those of copolymer films generated from a mixture of PFM and EGDA monomers at varying ratios. All characteristic peaks for both p(PFM) and p(EDGA) described above are present in the copolymer spectra without

exception. However, a close examination of the copolymer spectra reveals that the carbonyl bond absorptions associated with each independent material are shifted substantially. The p(PFM) carbonyl absorption, which appears at 1782 cm^{-1} in the pure polymer, appears at 1776 cm^{-1} in the 48% PFM copolymer. Additionally, the carbonyl absorption for p(EDGA), normally appearing at 1735 cm^{-1}, appears at 1741 cm^{-1} within this same copolymer. These shifts are indicative of coupling between the two carbonyl absorptions in the copolymer and would not be observed were the materials merely co-deposited[21].

Given that the spectra in Figure 4-2 have been thickness corrected, the intensity of a given IR absorption is directly proportional to the number of bonds absorbing at that frequency under the assumption that oscillator strength is constant. Indeed, this assumption has been verified for other iCVD copolymers[16]. Therefore, the ratio of PFM units to EGDA units within the copolymer was calculated through numerical fitting of the peak areas associated with absorptions unique to each material. In this work, the benzene C-C absorption (1523 cm^{-1}) has been selected as indicative of the PFM units and the C=O absorption (1741 cm^{-1}) of di-ester carbonyl as indicative of the EGDA units. This methodology yields a 48% PFM: 52% EDGA (±3%) composition from the 2nd spectra in Figure 1, and a 23% PFM: 77% EDGA (±3%) from the 3rd. Note that the ratios of PFM to EDGA incorporated in the films do not correspond to the ratios at which the two monomers are fed in the gas phase, 5:1 and 3:1 respectively. For iCVD polymerizations, the incorporation ratio in the copolymer is controlled by the respective vapor pressures of the two monomers at the temperature of the substrate and their relative polymerization reactivities, in addition to gas phase composition[16, 21].

4.4.2 Bulk Polymer Functionalization

As shown in the scheme of Figure 4-1, the pentafluorophenyl ester moiety present in p(PFM) and its copolymer with EGDA is highly reactive toward nucleophilic substitution[11-13]. This reactivity allows for single step functionalization of the copolymer by any nucleophilic agent, either small molecules or larger bio-active ones such as peptides. This property is demonstrated in Figure 4-3, which displays the IR spectrum of a copolymeric film (48% PFM: 52% EDGA) functionalized with 2,2-aminoethoxy ethanol (AEE). The IR spectrum of the unfunctionalized copolymer is also included for comparison. Within the IR spectrum of the functionalized material, the absorption peaks associated with the fluorinated phenyl ring (1523 cm^{-1}, 1000 cm^{-1}) are significantly reduced due to substitution of this group by the AEE. Analysis of the thickness corrected peak area associated with the C-C bonds within the phenyl ring (1523 cm^{-1}) indicates an 80% reduction in this moiety. In addition, four new peaks are apparent within the spectrum. The first, a broad peak centered at 3400 cm^{-1}, is indicative of the presence of the hydroxyl group of the AEE, specifically a hydrogen bonded O-H stretch[20]. Further evidence of the hydroxyl group is found at 1132 cm^{-1}, an absorption associated with the C-OH stretch. The two other added absorptions, at 1660 cm^{-1} and 885 cm^{-1}, are evidence of the amine moiety within that added AEE [20]. In addition, further evidence of AEE functionalization of the copolymer is apparent in contact angle measurements.

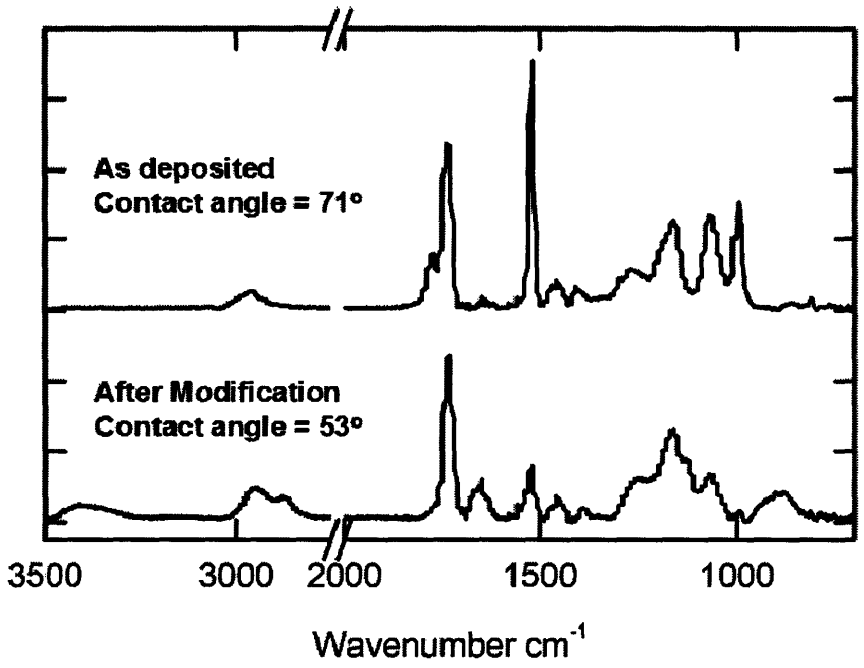

Figure 4-3. IR spectra of p(PFM-co-EGDA) both as deposited and after functionalization with aminoethoxy-ethanol. This single step modification exchanges the hydrophilic aminoethoxy-ethanol molecule for the hydrophobic pentafluorophenyl side chain moiety within the copolymer resulting in an 18° reduction in contact angle.

As indicated in Figure 4-3, the contact angle of the unmodified copolymer is 71 ° (±4 °), while the contact angle of the AEE modified film is reduced to 53° (±3 °). This reduction is a product of both the removal of the extremely hydrophobic fluorinated phenyl moiety and the addition of hydrophilic hydroxyl and amine moieties. It should be noted that functionalization of this film provides further evidence that the material is copolymer and not merely a mixed deposition of two homopolymers. Modification of pure p(PFM) films with AEE was also attempted as part of this work. However, it was observed that these films, once modified, dissolved entirely in the ethanol. As solubility in ethanol was not observed for unmodified p(PFM) films, it is hypothesized that the substitution of AEE for the fluorinated phenyl moiety induced this change in solubility, leading to complete dissolution of the films. Copolymeric films of p(PFM) and

p(EDGA) do not experience this solubility change, losing no thickness in ethanol after AEE modification. Were these films co-deposited homopolymers, loss of film thickness due to changes in p(PFM) solubility would be expected.

4.4.3 Patterned Polymer Functionalization

Many applications of immobilized bio-molecules also require their localization or patterning. Due to the reactivity of its fluorinated phenyl ester, p(PFM-co-EGDA) provides a substrate which is readily patterned with covalently attached molecules through microcontact (μCp) printing. Figure 4-4 displays an optical micrograph of a patterned copolymeric film under FITC fluorescent illumination. This film was patterned with fluorescein-5-thiosemicarbazide, an amine containing molecule which fluoresces under FITC illumination, applied from a PDMS μCp stamp containing an array of 100 μm circles. The fluorescent pattern remains even after repeated solvent rinses, indicating that the nucleophilic amine functionality within the fluorescein-5-thiosemicarbazide has reacted with the PFM and become immobilized. Stamping and rinsing of an uncoated substrate results in no fluorescent pattern, confirming that the amine-pentafluorophenyl ester reaction is required for immobilization. This experiment provides proof of concept for patterned functionalization of the copolymer; bioactive nucleophilic ligands could be immobilized on the surface in much the same manner.

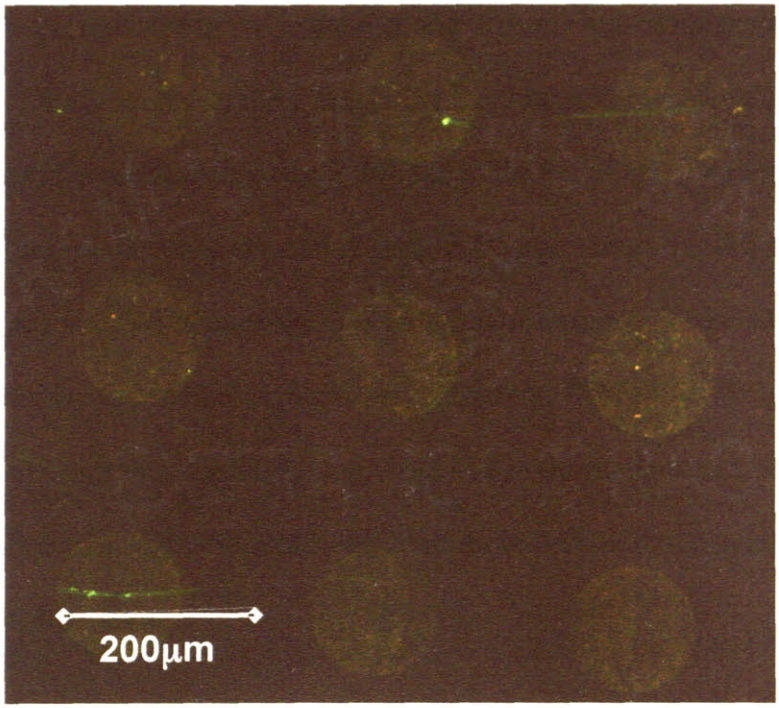

Figure 4-4. Copolymer film functionalized through microcontact printing of fluorescein-5-thiosemicarbazide. Fluorescent ligand remains immobilized after multiple solvent rinses, indicating that amine moieties within the ligand have reacted with the pentafluorophenyl ester present in the PFM side chains.

4.5 Conclusion

In this chapter, both deposition and functionalization of iCVD synthesized p(PFM-co-EDGA) films has been demonstrated. The structures of both the homopolymers, as well as the copolymer, have been verified through spectroscopy. In addition, both spectroscopic evidence and changes in material solubility indicate that the iCVD deposited material is indeed a copolymer, not merely a co-deposition of two separate polymers. Both bulk and patterned surface functionalization of the copolymer have been demonstrated through the addition of nucleophilic ligands. Bulk chemical modification was verified through spectroscopy which demonstrated the addition of

amine and hydroxyl moieties to the material along with the loss of the pentafluorophenyl leaving group. This functionalization was further confirmed through contact angle measurements, with a reduction of nearly 20° due to the exchange of hydrophilic for hydrophobic groups in the polymer side chains. Patterned surface modification, on the 100 μm scale, was verified through the attachment of fluorescently labeled amines which remained immobilized even after repeated solvent rinses. While this work utilized small nucleophilic molecules to establish the ease with which the material can be modified, future work will demonstrate the copolymer's utility in immobilizing peptides for cell adhesion and proliferation.

4.6 Acknowledgement

The authors acknowledge support of the NIH, under funding contract #NO1-NS2-2347, and support in part by the U.S. Army through the Institute for Soldier Nanotechnologies, under Contract DAAD-19-02-D-0002 with the U.S. Army Research Office. Nuria Mari-Buye, acknowledges financial support from the Generalitat de Catalunya under a Grant 2006FI 00447 of the Agència de Gestió d'Ajuts Universitaris i de Recerca (AGAUR).

4.7 References

1. Lahann, J., Vapor-based polymer coatings for potential biomedical applications. *Polymer International* **2006,** 55, (12), 1361-1370.
2. Siow, K. S.; Britcher, L.; Kumar, S.; Griesser, H. J., Plasma methods for the generation of chemically reactive surfaces for biomolecule immobilization and cell colonization - A review. *Plasma Processes And Polymers* **2006,** 3, (6-7), 392-418.
3. Guo, K. T.; Schafer, R.; Paul, A.; Gerber, A.; Ziemer, G.; Wendel, H. P., A new technique for the isolation and surface immobilization of mesenchymal stem cells from whole bone marrow using high-specific DNA aptamers. *Stem Cells* **2006,** 24, (10), 2220-2231.

4. Beckstead, B. L.; Santosa, D. M.; Giachelli, C. M., Mimicking cell-cell interactions at the biomaterial-cell interface for control of stem cell differentiation. *Journal Of Biomedical Materials Research Part A* **2006,** 79A, (1), 94-103.
5. Nakajima, M.; Ishimuro, T.; Kato, K.; Ko, I. K.; Hirata, I.; Arima, Y.; Iwata, H., Combinatorial protein display for the cell-based screening of biomaterials that direct neural stem cell differentiation. *Biomaterials* **2007,** 28, (6), 1048-1060.
6. Christenson, E. M.; Wiggins, M. J.; Anderson, J. M.; Hiltner, A., Surface modification of poly(ether urethane urea) with modified dehydroepiandrosterone for improved in vivo biostability. *Journal Of Biomedical Materials Research Part A* **2005,** 73A, (1), 108-115.
7. Massia, S. P.; Holecko, M. M.; Ehteshami, G. R., In vitro assessment of bioactive coatings for neural implant applications. *Journal Of Biomedical Materials Research Part A* **2004,** 68A, (1), 177-186.
8. Blankenstein, G.; Larsen, U. D., Modular concept of a laboratory on a chip for chemical and biochemical analysis. *Biosensors & Bioelectronics* **1998,** 13, (3-4), 427-438.
9. Kim, H.; Doh, J.; Irvine, D. J.; Cohen, R. E.; Hammond, P. T., Large area two-dimensional B cell arrays for sensing and cell-sorting applications. *Biomacromolecules* **2004,** 5, (3), 822-827.
10. Schofield, W. C. E.; McGettrick, J. D.; Badyal, J. P. S., A substrate-independent approach for cyclodextrin functionalized surfaces. *Journal Of Physical Chemistry B* **2006,** 110, (34), 17161-17166.
11. Francesch, L.; Garreta, E.; Balcells, M.; Edelman, E. R.; Borros, S., Fabrication of bioactive surfaces by plasma polymerization techniques using a novel acrylate-derived monomer. *Plasma Processes And Polymers* **2005,** 2, (8), 605-611.
12. Lahann, J.; Balcells, M.; Lu, H.; Rodon, T.; Jensen, K. F.; Langer, R., Reactive polymer coatings: A first step toward surface engineering of microfluidic devices. *Analytical Chemistry* **2003,** 75, (9), 2117-2122.
13. Lahann, J.; Balcells, M.; Rodon, T.; Lee, J.; Choi, I. S.; Jensen, K. F.; Langer, R., Reactive polymer coatings: A platform for patterning proteins and mammalian cells onto a broad range of materials. *Langmuir* **2002,** 18, (9), 3632-3638.
14. Francesch, L.; Borros, S.; Knoll, W.; Forch, R., Surface reactivity of pulsed-plasma polymerized pentafluorophenyl methacrylate (PFM) toward amines and proteins in solution. *Langmuir* **2007,** 23, (7), 3927-3931.
15. Yasuda, H., *Plasma Polymerization.* Academic Press: 1985.
16. Chan, K.; Gleason, K. K., Initiated chemical vapor deposition of linear and cross-linked poly(2-hydroxyethyl methacrylate) for use as thin-film hydrogels. *Langmuir* **2005,** 21, (19), 8930-8939.
17. Mao, Y.; Gleason, K. K., Hot filament chemical vapor deposition of poly(glycidyl methacrylate) thin films using tert-butyl peroxide as an initiator. *Langmuir* **2004,** 20, (6), 2484-2488.
18. O'Shaughnessy, W. S.; Gao, M. L.; Gleason, K. K., Initiated chemical vapor deposition of trivinyltrimethylcyclotrisiloxane for biomaterial coatings. *Langmuir* **2006,** 22, (16), 7021-7026.

19. Lyles, B. F.; Terrot, M. S.; Hammond, P. T.; Gast, A. P., Directed patterned adsorption of magnetic beads on polyelectrolyte multilayers on glass. *Langmuir* **2004,** 20, (8), 3028-3031.
20. D. Lin-Vien, N. C., W. Fately, J. Grasselli, *The Handbook of Infrared and Ramman Characteristic Frequencies of Organic Molecules*. Academic Press: San Diego, 1991.
21. Lau, K. K. S.; Gleason, K. K., All-Dry Synthesis and Coating of Methacrylic Acid Copolymers for Controlled Release. *Macromolecular Bioscience* **2007,** In Press.

Chapter Five

Additively Patterned Polymer Thin Films by Photo-Initiated Chemical Vapor Deposition (piCVD)*

* To be submitted.

5.1 Abstract

Micropatterened thin films have many applications in the fields of electronics and biomaterials. Traditional subtractive methods for creating patterned thin films are slow, costly, and environmentally unfriendly. In this work, a novel technique for the creation of patterned polymeric thin films is demonstrated. A free radical generating photo-initiator is first patterned on the substrate by microcontact printing. Patterned polymer thin films are then grown by exposing the initiator to UV irradiation in the presence of gaseous vinyl containing monomer at low pressure (250-300 mTorr). Using this technique, patterned films of poly(cyclohexyl methacrylate) are deposited with a resolution 100 m and a thickness of 250-300 nm. The versatility of this technique will allow its future use for deposition of chemically functional polymeric films with nanoscale features.

5.2 Introduction

Patterned thin films have applications in many fields, from microelectronics to biomaterials. Micro- and nano-scale structures are the basic building blocks of the semiconductor industry[1], essential for the manufacture of all modern electronics. They are also necessary for novel electronics applications such as organic electronics[2], flexible displays[3], and optical waveguides[4]. Patterned thin films have utility in both basic biological studies[5] and bio-implantable materials design[6]. Microstructure patterns on the surface of biomaterials can be used stimulate cell recognition and adhesion[6]. They also have utility for sorting of cell mixtures through controlling cell-surface interactions[7].

Traditionally, the creation of patterned thin films has been performed by subtraction, requiring the deposition of full layers of material which are then selectively removed to create the desired structures[8]. Often an additional photoresist layer, which can be patterned through UV irradiation, must also be deposited. Further steps area also required to develop the resist, transfer the pattern through the resist to the material below, and then remove the remaining resist. This process is slow, wasteful, and environmentally unfriendly due to the large volumes of solvent involved[9, 10]. In addition, a plasma etch process is often utilized for transferring the pattern from the resist to the underlying layer. This process can create damage in both the remaining material structures and the underlying substrate[11].

Additive processing of polymeric films by chemical vapor deposition (CVD) has been demonstrated by Yatsutake et. al. using substrates pre-patterned with thermally labile initiators[12]. Additionally, Andou et. al. have deposited additively patterned thin films from vapor phase monomers utilizing surface tethered photo-initiators activated by irradiation through a photo mask[13]. In this chapter, a novel approach for additive patterning of thin film structures is described and initial results utilizing this technique are presented. A free radical generating photo-initiator is first patterned onto the substrate using microcontact printing. This substrate is then exposed to UV irradiation, under vacuum, in the presence of a vaporized monomer in a process termed photo-initiated CVD (piCVD)[14]. For this work, cyclohexyl methacrylate (CHMA) has been selected as the monomer and benzophenone, or its derivative, as the photo-initiator. Previous work within our lab, demonstrating both polymerization of CHMA by initiated CVD[15, 16] and the photo-initiated CVD of other monomers with benzophenone[17] inspired

this selection of model system. pCHMA is an excellent sacrificial material and patterned films of this polymer have been utilized in the formation of air gap structures[16]. The approach described in this manuscript differs from the previous work of Yatsutake et. al. in that it allow the substrate to be maintained at room temperature. The technique also extends on the work of Andou et al. by allowing deposition of much thicker patterned films. These advantages will allow use of this technique for both biological applications, where temperature sensitive substrates may be involved, and microelectronic applications, where features of significant thickness are required. In addition, this work is the first example of additively patterned vapor deposited polymer films using soft lithography. The method is quite general and could deposit patterned films of any polymer that can be synthesized by initiated CVD including poly(glycidyl methacrylate)[18], poly(hydroxyethyl methacrylate)[19], poly(perfluorodecyl acrylate)[20], and poly(trivinyltrimethylcyclotrisiloxane)[21].

5.3 Experimental

5.3.1 Microcontact Stamp Preparation

In order to pattern photo-initiator onto silicon wafer substrates, poly(dimethyl siloxane) (PDMS) stamps were prepared with arrays of either 100 μm diameter circles or 100 X 200 μm rectangles. To form the stamps, liquid PDMS polymer was mixed with crosslinking agent (Sylgard 184, Dow Corning) and 35-50 g of the mixture poured over a silicon stamp master. Initially, a ratio of 10:1 PDMS to crosslinker was utilized, though this was decreased to 7:1 in order to create higher modulus stamps with superior performance for the application. The stamp master itself was prepared through

conventional lithography steps for a previous study[22]. The PDMS mixture was degassed under vacuum for one hour and then baked at 70 °C under vacuum for 12 hours. The solid PDMS stamp was then removed from the master and sectioned for use.

5.3.2 Silicon Wafer Surface Preparation

Silicon wafers (Waferworld) were utilized as substrates for all patterned depositions. Experiments were performed on unmodified wafers which were blown clean with room temperature nitrogen prior to photo-initiator stamping. Hydrophobic substrates, presenting phenyl moieties, were prepared as follows. First, a silicon wafer was treated with 0.32W/cm^2 radio frequency discharge oxygen plasma for 10 minutes. Oxygen pressure was maintained at 200 mtorr at a flowrate of 10 sccm. The wafer was maintained at 35 °C though backside cooling The treated wafer was then placed in a vacuum desiccator along with an open flask containing 0.5 – 1 ml of trichlorophenyl silane (97%, Aldrich). The desiccator was evacuated to vacuum and sealed for 90 minutes. Following this step, the wafer was dipped in toluene to remove any unreacted silane and dried with room temperature nitrogen.

5.3.3 Initiator Stamping

Solutions of benzophenone (BP) (99%, Alfa Aesar) in acetone (99.5%, Aldrich) were generated at 0.1%, 1%, and 10% by weight. Solutions of 4-4-Bis(dimethylamino) benzophenone (Michler's Ketone, MK) (99%, Fluka) in acetone were generated at 0.1%, 1%, and 2.2% (saturation) by weight. Each solution was applied to the surface of the PDMS microcontact stamp with a cotton swab. Stamps were either applied directly to

the silicon wafer substrate for 60 seconds, or dried with room temperature nitrogen then applied to the substrate. Table 5-1 shows the combinations of initiator, concentration, and substrate utilized for each deposition.

5.3.4 Patterned Film Deposition

Following initiator microcontact stamping, wafer substrates were immediately placed into a custom built iCVD deposition chamber, as has been previously described in detail[18, 19]. Cyclohexyl methacrylate (97%, Aldrich) was vaporized in a metal crucible at a tempertature of 70 °C and metered into the reactor at a rate of 2 sccm through a vapor flow controller (MKS model 1152). Pressure within the chamber was measured by a capacitance diaphragm gauge and controlled at values ranging from 200 – 300 mTorr through use of a throttling butterfly valve (Intellisys, NorCal) connected to an auto-tuned digital controller (Intellisys, NorCal). Once reactor pressure was stabilized, substrates were irradiated with UV light at either 254 or 365 nm (6 watt handheld UV lamp, UVP) wavelengths for 45 minutes. Throughout the deposition, wafer temperature was maintained at 35 °C by backside circulation of cooling water below the substrate stage. A complete listing of reactor condition combinations utilized is shown in Table 5-1.

Sample Name	Initiator	Solution Concentration (wt%)	Stamped Wet or Dry	Substrate Treatment	Pressure (mTorr)	UV Wavelength (nm)
A	BP	5.0	Dry	None	250	254
B	BP	5.0	Wet	None	250	254
C	MK	0.1	Dry	PS	250	254
D	MK	1.0	Dry	PS	250	254
E	MK	2.2 (sat.)	Dry	PS	250	254
F	MK	2.2 (sat.)	Dry	PS	300	254
G	MK	2.2 (sat.)	Dry	PS	300	365

Table 5-1. Experimental conditions utilized to produce samples discussed in this study. Note that (sat.) refers to MK at its saturation condition in acetone (~2.2 wt%). Wet or dry refers to whether or not the PDMS stamp was blown dry with nitrogen prior to contacting the substrate. PS refers to trichlorophenyl silane treatment of the substrate.

5.3.5 Sample Analysis

Deposited films were analyzed optically using an Olympus CX41 optical microscope with attached digital camera. In all cases, optical microscopy was performed after initiator stamping and also after after polymer deposition to ensure observed patterns were due to polymer film growth. Scanning electron micrographs were obtained on a JEOL 5910 General Purpose Scanning Electron Microscope (SEM) at acceleration voltages of 2.5-10 kV. Samples were coated with 5-10 nm of gold using an evaporator (Desk II, Denton Vacuum) prior to SEM examination. Deposited film thicknesses were measured using a Tencor P-10 Surface Profilometer.

5.4 Results and Discussion

Initial experiments designed for creating additively patterned polymer films were performed through microcontact stamping of benzophenone (BP) dissolved in acetone. BP is a type II free radical initiator which can be activated with both 254 and 365 nm wavelength UV photons[23]. In addition, the low vapor pressure of BP (< 3 mTorr at 298K)[24] allowed samples to be placed under vacuum without expectation of initiator pattern evaporation. Representative results of patterned deposition resulting from photo-initiated CVD (piCVD) of CHMA on substrates to which the microcontact stamp was applied without drying are shown in Figure 5-1. This figure corresponds to condition "B" from Table 5-1. Some patterned polymer growth is evident, though only corresponding to the outline of the microcontact stamp feature. This phenomenon, observed in inkjet printing of microscale features[3, 25], is commonly termed the 'coffee drop' effect. It is the result of the BP solution concentrating during evaporative drying of the more volatile acetone. Retention of pattern edge fidelity occurs due to surface tension and wetting effects which dictate that the evaporative front move from the center of the wetted area to the edge[26]. The intentional use of this phenomenon to create patterns, known as edge transfer lithography (ETL), has been shown to allow the transfer of smaller features than traditional microcontact printing[27]. This may indicate that utilization of this process for additive patterning is a possibility. However, while depositions on substrates patterned with BP in this manner do create line features of 2-3 μm in width, as shown in Figure 5-1b, the process is not highly reproducible, as evidenced by the lack of regularity of the pattern in Figure 5-1a. Therefore, in order to reliably create additive patterns, full depositional coverage of patterned areas is desirable.

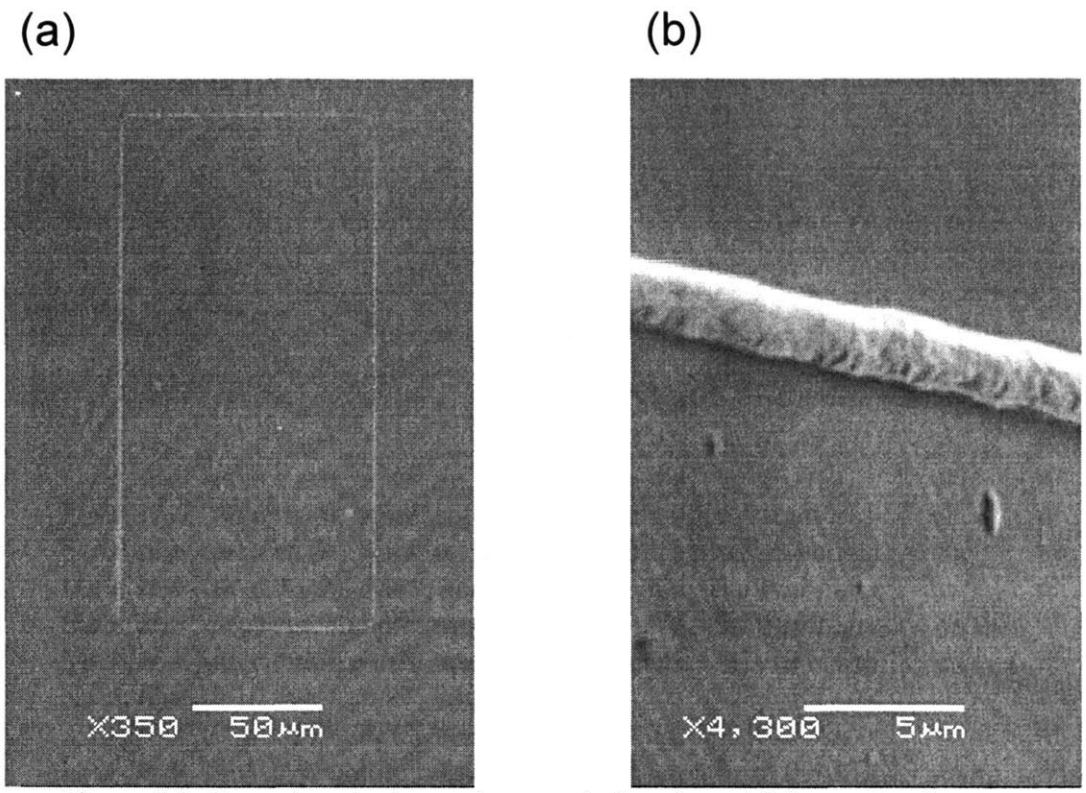

Figure 5-1. Scanning electron micrograph showing additive patterning achieved by deposition of piCVD CHMA following microcontact printing of BP/acetone solution, showing (a) the outline of a 100 µm X 200 µm rectangle resulting from concentration of the BP at the edge of the feature as the acetone evaporated and (b) an enlargement of one edge of the deposited structure.

It should be noted that when the microcontact stamp was dried with nitrogen prior to contacting the substrate (condition "A", Table 5-1), no deposition was observed. Instead, visual inspection revealed that crystallization of the BP occurred on the surface of the PDMS stamp. BP is a highly crystalline solid at room temperature, and the formation of large BP crystals on the face of the stamp likely prevented the transfer of any initiator to the substrate. To avoid this issue, 4-4-bis(dimethylamino)benzophenone, commonly known as Mickler's Ketone (MK), was substituted for BP as the photo-initiating species. The structure of MK is identical to that of BP, as shown schematically

in Figure 5-2, but with the addition of two di-methyl amino groups. MK is therefore still activated at the same UV wavelengths as BP but is much less prone to crystallization.

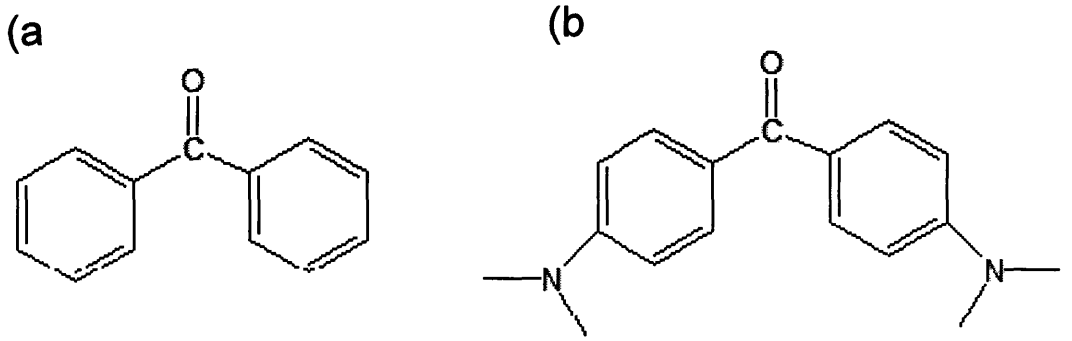

Figure 5-2. Schematic representation of the chemical structures of (a) benzophenone and (b) Mickler's Ketone. Both initiators activate at the same UV wavelengths due to the carbonyl joining the two phenyl moieties. However, the presence of the dimethylamino side groups on the Michler's Ketone make this structure significantly less likely to crystallize.

In order to further promote transfer of the initiator from the PDMS stamp, surface modification of the substrate with trichlorophenyl silane was performed, as shown schematically in Figure 5-3. It was hypothesized that the presence of phenyl rings on the substrate surface would create favorable interactions with those present in the MK. Initial experiments performed with low concentration solutions of MK (conditions "C" and "D" in Table 5-1) resulted in 'coffee drop' structures (not shown) similar to those resulting from wet stamping of BP. In this case, the 'coffee ring' effect occurred on the surface of the PDMS stamp as the applied MK/ acetone solution was dried with nitrogen prior to substrate contacting. These results indicated that MK present on the stamp surface was transferring to the substrate and subsequently initiating CHMA polymer deposition.

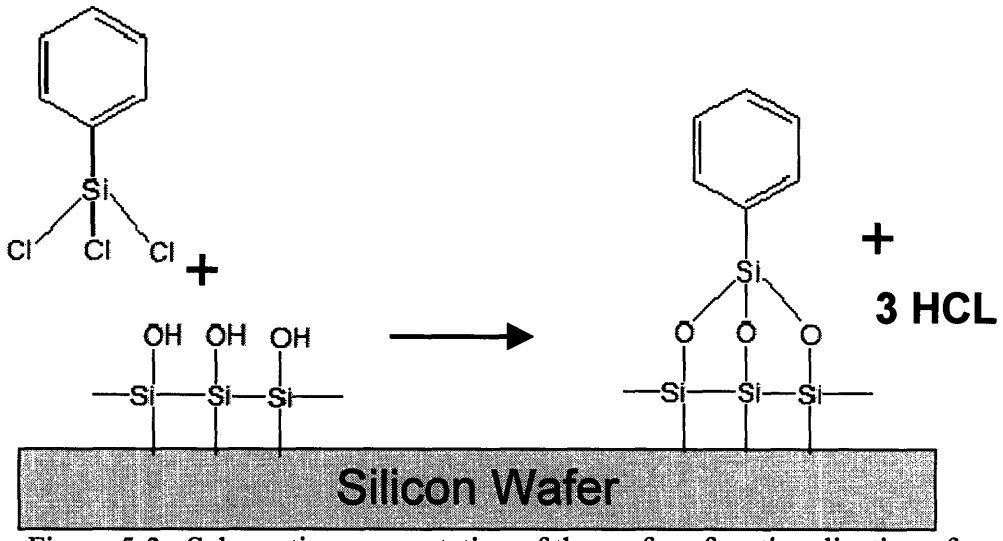

Figure 5-3. Schematic representation of the surface functionalization of asilicon wafer substrate with trichlorophenyl silane. The surface attached phenyl rings create favorable interations with those present in MK, leading to increase transfer of initiator during microcontact printing.

Figure 5-4 displays an optical micrograph of a patterned CHMA film deposited using condition "E" in Table 5-1. As is observed in the figure, depositional coverage over the full area patterned by the initiator has been achieved. It is theorized that by utilizing a solution of MK in acetone at its saturation concentration, the initiator was forced to precipitate on the stamp surface during solvent evaporation. This led to complete coverage of the stamp area with MK, which then transferred to the substrate during contacting due to favorable interactions with phenyl modified surface.

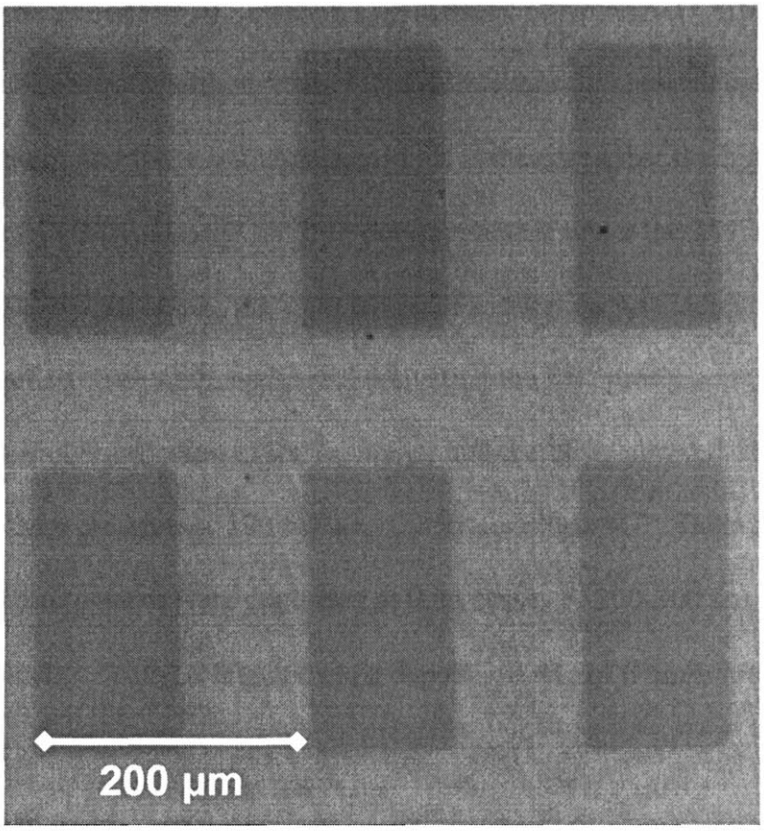

Figure 5-4. Optical micrograph of 100 µm X 200 µm features deposited through piCVD of pCHMA which formed after microcontact patterning with the MK initiator. Full feature area is filled in while deposition is not apparent outside of initiator patterned area.

It should be noted that the features shown in Figure 5-4 have a thickness of 25-30 nm, as measured by surface profilometry. This corresponds to a film deposition rate of only ~0.5 nm/minute. Many applications of patterned thin films, especially those in the microelectronics industry, require significantly larger film thicknesses. In order to achieve thicker patterned films on reasonable time scale, deposition rates at least an order of magnitude higher are required. One common approach for increasing film growth rates in iCVD is to increase the partial pressure of the monomer within the deposition chamber[15, 28, 29]. This in turn increases the surface concentration of adsorbed monomer and therefore the rate of polymerization[28, 29]. However, when CHMA pressure was increased from 250 mTorr to 300 mTorr under 254 nm UV illumination, patterned

growth was no longer observed. Instead, a continuous polymerized CHMA film was deposited on the substrate, with no observable differentiation between areas patterned with photo-initiator and those left unpatterned. It is theorized that the higher surface concentration of CHMA allowed for auto-polymerization under the 254 nm UV irradiation. To avoid this issue, the wavelength of irradiation was increased to 365 nm. This less energetic wavelength, while still activating the MK present on the surface, did not initiate auto-polymerization of the monomer and therefore allowed for patterned film growth at a CHMA pressure of 300 mTorr. Under condition "G", Table 5-1, patterned films with 100 μm features were deposited at thicknesses of 250-300 nm, as measured by surface profilometry. This corresponds to a deposition rate of 6 nm/minute.

5.5 Conclusion

In this work, the deposition of patterned polymeric thin films of p(CHMA) has been demonstrated. By microcontact printing photo-initiator onto silicon wafer substrates pretreated with trichlorophenyl silane, then exposing these substrates to 365 nm UV irradiation in the presence of CHMA monomer, features with 100 μm resolution and film thicknesses of 250-300 nm have been achieved. As the piCVD technique does not depend of the method of initiator application nor the specific side chain moieties of the vinyl monomer, many options exist for the extension of this approach in depositing patterned thin films. In future work, alternate lithography approaches, such as photo-bleaching of a blanket initiator layer through interference lithography will be examined for the creation smaller patterned features. In addition, alternate monomers such as

glycidyl methacrylate or pentafluorophenyl methacryalte will be utilized to deposited patterned thin films of functional polymers for biological applications.

5.6 Acknowledgement

The authors acknowledge support of both the ERC/Sematech Research Center for Environmentally Benign Semiconductor Manufacture and the National Science Foundation. The authors would also like to thank Prof. Paula Hammond's lab at MIT for use of microcontact printing materials.

5.7 References

1. May, G. S., *Fundamentals of Semiconductor Manufacturing and Process Control.* Wiley-Interscience: Hoboken, NJ, 2006.
2. Kelley, T. W.; Baude, P. F.; Gerlach, C.; Ender, D. E.; Muyres, D.; Haase, M. A.; Vogel, D. E.; Theiss, S. D., Recent progress in organic electronics: Materials, devices, and processes. *Chemistry Of Materials* **2004,** 16, (23), 4413-4422.
3. Street, R. A.; Wong, W. S.; Ready, S. E.; Chabinyc, I. L.; Arias, A. C.; Limb, S.; Salleo, A.; Lujan, R., Jet printing flexible displays. *Materials Today* **2006,** 9, (4), 32-37.
4. Chang, C. C.; Chen, C. P.; Chou, C. C.; Kuo, W. J.; Jeng, R. J., Polymers for electro-optical modulation. *Journal Of Macromolecular Science-Polymer Reviews* **2005,** C45, (2), 125-170.
5. Whitesides, G. M.; Ostuni, E.; Takayama, S.; Jiang, X. Y.; Ingber, D. E., Soft lithography in biology and biochemistry. *Annual Review Of Biomedical Engineering* **2001,** 3, 335-373.
6. Sardella, E.; Favia, P.; Gristina, R.; Nardulli, M.; d'Agostino, R., Plasma-aided micro- and nanopatterning processes for biomedical applications. *Plasma Processes And Polymers* **2006,** 3, (6-7), 456-469.
7. Alexeev, A.; Verberg, R.; Balazs, A. C., Patterned surfaces segregate compliant microcapsules. *Langmuir* **2007,** 23, (3), 983-987.
8. Bucknall, D. G., *Nanolithography and patterning techniques in microelectronics.* Woodhead Publishing: Cambridge, 2005.
9. *1997 Semiconductor Industry Association National Technology Roadmap for Semiconductors.*
10. *1996 Electronics Industry Environmental Roadmap (EEIR).*
11. Yasuda, H., *Plasma Polymerization.* Academic Press: 1985.
12. Yasutake, M.; Hiki, S.; Andou, Y.; Nishida, H.; Endo, T., Physically controlled radical polymerization of vaporized vinyl monomers on surfaces. Synthesis of block

copolymers of methyl methacrylate and styrene with a conventional free radical initiator. *Macromolecules* **2003,** 36, (16), 5974-5981.
13. Andou, Y.; Nishida, H.; Endo, T., Designed surface construction by photo-induced vapor-phase assisted surface polymerization of vinyl monomers using immobilized free radical initiators. *Chemical Communications* **2006,** (48), 5018-5020.
14. Chan, K.; Gleason, K. K., Photoinitiated chemical vapor deposition of polymeric thin films using a volatile photoinitiator. *Langmuir* **2005,** 21, (25), 11773-11779.
15. Chan, K.; Gleason, K. K., A mechanistic study of initiated chemical vapor deposition of polymers: Analyses of deposition rate and molecular weight. *Macromolecules* **2006,** 39, (11), 3890-3894.
16. Chan, K.; Gleason, K. K., Air-gap fabrication using a sacrificial polymeric thin film synthesized via initiated chemical vapor deposition. *Journal Of The Electrochemical Society* **2006,** 153, (4), C223-C228.
17. Martin, T. M.; Sedransk, K.; Chan, K.; Baxamusa, S.; Gleason, K. K., Solventless Surface Photoinitiated Polymerization: Grafting Chemical Vapor Deposition (gCVD). *Macromolecules* **2007,** In Press.
18. Mao, Y.; Gleason, K. K., Hot filament chemical vapor deposition of poly(glycidyl methacrylate) thin films using tert-butyl peroxide as an initiator. *Langmuir* **2004,** 20, (6), 2484-2488.
19. Chan, K.; Gleason, K. K., Initiated chemical vapor deposition of linear and cross-linked poly(2-hydroxyethyl methacrylate) for use as thin-film hydrogels. *Langmuir* **2005,** 21, (19), 8930-8939.
20. Gupta, M.; Gleason, K. K., Initiated chemical vapor deposition of poly(1H,1H,2H,2H-perfluorodecyl acrylate) thin films. *Langmuir* **2006,** 22, (24), 10047-10052.
21. O'Shaughnessy, W. S.; Gao, M. L.; Gleason, K. K., Initiated chemical vapor deposition of trivinyltrimethylcyclotrisiloxane for biomaterial coatings. *Langmuir* **2006,** 22, (16), 7021-7026.
22. Lyles, B. F.; Terrot, M. S.; Hammond, P. T.; Gast, A. P., Directed patterned adsorption of magnetic beads on polyelectrolyte multilayers on glass. *Langmuir* **2004,** 20, (8), 3028-3031.
23. Mishra, M. K., *Handbook of Radical Vinyl Polymerization.* Marcel Dekker: New York, 1998.
24. Monte, M. J. S.; Santos, L.; Fulem, M.; Fonseca, J. M. S.; Sousa, C. A. D., New static apparatus and vapor pressure of reference materials: Naphthalene, benzoic acid, benzophenone, and ferrocene. *Journal Of Chemical And Engineering Data* **2006,** 51, (2), 757-766.
25. Tekin, E.; de Gans, B. J.; Schubert, U. S., Ink-jet printing of polymers - from single dots to thin film libraries. *Journal Of Materials Chemistry* **2004,** 14, (17), 2627-2632.
26. Deegan, R. D.; Bakajin, O.; Dupont, T. F.; Huber, G.; Nagel, S. R.; Witten, T. A., Capillary flow as the cause of ring stains from dried liquid drops. *Nature* **1997,** 389, (6653), 827-829.
27. Woodson, M.; Liu, J., Functional nanostructures from surface chemistry patterning. *Physical Chemistry Chemical Physics* **2007,** 9, (2), 207-225.

28. Lau, K. K. S.; Gleason, K. K., Initiated chemical vapor deposition (iCVD) of poly(alkyl acrylates): An experimental study. *Macromolecules* **2006,** 39, (10), 3688-3694.
29. Lau, K. K. S.; Gleason, K. K., Initiated chemical vapor deposition (iCVD) of poly(alkyl acrylates): A kinetic model. *Macromolecules* **2006,** 39, (10), 3695-3703.

Chapter Six

Conclusions and Future Work

6.1 Conclusions

In this thesis, novel polymers for insulation and biopassivation of neural recording electrodes have been developed and their properties verified. In order to maximize coating efficacy, two separate materials were synthesized. The first, poly(V_3D_3), is a flexible, electrically insulating polymer for encapsulation and protection of the microelectronic probes. Initial biocompatibility of this insulating material has been verified, along with long term electrical property retention under simulated physiological conditions. The second material, p(PFM-co-EGDA), is a functional polymer which serves as a platform for surface modification of probe coatings with bioactive moieties such as adhesion peptides. Both these materials were synthesized through initiated chemical vapor deposition, an ideal methodology for the conformal coating of high aspect ratio substrates possessing nano-scale features. The sequential deposition of these two polymers will provide the bulk and surface properties required to both protect the neural probe from the biological environment of the central nervous system and stabilize its interactions with said environment.

In addition to these two materials, a novel technique for the additive patterning of CVD deposited polymeric thin films has been developed. This technique will allow the physical patterning of biomaterial coatings to maximize biocompatibility. The method also has applications in the manufacture of semiconductors.

6.1.1 Synthesis of poly(trivinyltrimethylcyclotrisiloxane)

A novel insulating polymeric material has been developed for the insulation of implantable microelectronics *in vivo*. The polymer, poly(trivinyltrimethyl-cyclotrisiloxane) (poly(V_3D_3)), is a highly crosslinked matrix material formed through initiated chemical vapor deposition. The structure of this polymer has been verified through the use of FTIR and XPS spectroscopy. These data confirm that the polymer is formed through free radical polymerization of pendant vinyl groups present on the monomer and that these groups are almost entirely consumed by this reaction. In addition, the structure of the polymer retains all other moieties, aside from the vinyl, present in the monomer. The chemical structure of the material indicates that the polymerization chemistry is limited to only a single reaction pathway. Average polymer

backbone length has been estimated to be 8.9 units, based on XPS spectroscopy. However, as each monomer unit participates in three separate backbone chains the molecular weight of the polymer is immeasurably large (due to insolubility). The kinetic properties of the iCVD deposition process for this material have also explored. Effective activation energies of 28 kJ/mol, with respect to filament temperature, and -23.2 kJ/mol, with respect to substrate temperature, were obtained.

6.1.2 Material Property Characterization of poly(V_3D_3)

The physical and electrical properties of poly(V_3D_3) have been explored and its suitability as a thin film insulating material verified. Poly(V_3D_3) has a bulk electrical resistivity in excess of 10^{15} Ω–cm, allowing for films as thin as 5μm to provide the required degree of electrical insulation for the application. It has been shown to be flexible through SEM examination of stressed wire coatings. The material's RMS surface roughness has been found to be only 0.4 nm with a peak to peak roughness of <0.9 nm. This polymer is hydrolytically stable, as demonstrated by FTIR of soak tested samples, and insoluble in all tested solvents. Thin films of the material also show excellent adhesion to silicon substrates, with no delamination apparent by ASTM tape test, even after samples are boiled in deionized water. In addition, a hypothesis that this polymer would behave as a hybrid of polyethylene and a poly(siloxane) has been verified through comparison of physical and electrical properties.

Subsequent to characterization of the material properties of as-deposited poly(V_3D_3) films, long term stability of the electrical properties has been verified. Soak testing under physiological conditions for over 1000 days was performed with no observed loss of electrical resistivity. In addition, initial biocompatibility with PC12 neurons has been demonstrated, indicating that poly(V_3D_3) is not cytotoxic to these cells.

6.1.3 Synthesis and functionalization of poly(PFM-co-EGDA)

In order to provide for the facile attachment of bioactive molecules, specifically peptides, a copolymer of pentalfuorophenylmethacrylate (PFM) and ethylene glycol diacrylate (EGDA) has been synthesized by iCVD. This material is a crosslinked functional polymer which can act as a platform for attachment of biomolecules through

single step nucleophilic substitution. Both the homopolymer of PFM and a range of PFM-co-EDGA polymer compositions have been demonstrated with both spectroscopic and physical (insolubility) evidence of copolymerization. Bulk solution functionalization of the material by a small molecule amine has been performed. The resulting material displays a >80% reduction in the pentafluorophenyl ester, as estimated from FTIR, and a decrease in contact angle from 71° to 53°. Patterned surface functionalization of the material through microcontact printing of fluorescent amines has also been demonstrated, with features of 100μm resolution.

6.1.4 Additive patterning of poly(cyclohexylmethacrylate)

As the final element of this thesis, a novel technique for the chemical vapor deposition of additively patterned thin films has been developed. This technique utilizes benzophenone, or one of its derivatives, as a photo-active initiator to drive free radical polymerization of a vinyl monomer. The photo-initiator is localized on the substrate through microcontact printing, where it remains due to vapor pressure considerations, prior to CVD deposition. When the substrate is subsequently activated with UV irradiation in the presence of gaseous monomer, a patterned film is deposited. Using cyclohexyl methacrylate as a model system, patterned features of 100 μm resolution were deposited at a film thickness of >200 nm. The importance of pre-treating the substrate surface prior to microcontact printing of the initiator was also investigated. Superior depositional feature fidelity was found when the substrate was pretreated with trichlorophenylsilane.

6.2 Future Work

Within this thesis, a strategy has been set forth to address the requirements for biopassivation of neurological implants and materials have been designed to meet these requirements. However, as with any scientific investigation, further optimization steps are possible and may be required before clinical application of these materials. Data obtained on poly(V_3D_3) indicates that it has excellent material stability and is not cytotoxic to neurons. The next logical step is to coat a neural probe with this material and implant it in an animal model. Work to this effect with a rabbit model was planned

in collaboration with Innersea Technology Inc. but unfortunately was not carried out due tofunding issues (NIH funding for such studies was not renewed). In addition, poly(V_3D_3) deposits quite slowly for an iCVD material, likely too slowly to be manufacturable. Further investigations should be performed in order to increase this deposition rate without negatively affecting the bulk properties of the material. One approach would be to copolymerize the V_3D_3 with a small mono-vinyl molecule. This co-monomer could act as a spacer molecule to reduce the steric hindrance associated with the reaction of two large V_3D_3 rings. Work to this effect is planned through GVD corporation, an iCVD startup company in Cambridge, MA. They have received a Phase II SBIR form the NIH for development of a related coating and will also likely receive a phase I SBIR for the further development of this exact formulation.

Further development work with poly(PFM-co-EGDA) could also be performed. One step would be the modification of this material with bioactive ligands, such as laminin and L1, and subsequent biocompatibility testing with neurons, astrocytes, and glial cells. A ready collaborator for such studies would be Prof. Shashi Murthy of Northeastern University. These experiments would further validate the material's utility for promoting central nervous system cell adhesion and could also elucidate methods for patterning surface ligands on neural probes to maximize probe viability *in vivo*. Another useful extension would be the creation of a PFM - V_3D_3 copolymer. Ideally, PFM could be graded into the composition of the material near the surface of the coating so as to make for one continuous deposition. This approach would have multiple advantages, including better material stability, versus two independent coating layers and may allow for the elimination of EGDA as a comonomer.

Lastly, the additive patterning work presented in chapter five could be further extended to allow for deposition of smaller features. One approach for achieving this would be to change the lithographic technique used for initiator patterning. An alternate approach which may allow for features on the 100 nm scale would be photo-bleach patterning through interference lithography. In this approach, the photo-initiator would be applied as a blanket layer to the substrate, possible by spin-on from solvent. After drying, but prior to deposition, the substrate could then be exposed to patterned UV light at a very energetic wavelength (188 nm). This exposure would deactivate the irradiated

initiator, leaving a negative pattern that could then be utilized to deposit additively patterned polymer films as in the current approach. Additionally, the initiator could be covalently tethered to the substrate which may increase pattern resolution by preventing initiator diffusion during deposition. These steps are planned work for a new graduate student, Nathan Trujillo, who has recently joined the Gleason lab. Synthesis of tethered initiator molecules will be carried out in collaboration with Dr. Chris Ober of Cornell University.